

ENGINEERING EXPERIMENT STATION
of the Georgia Institute of Technology
Atlanta, Georgia

FINAL REPORT

PROJECT NO. B-207

INTERACTION OF SUBMICRON SMOG PARTICLES AND VAPORS

By

CLYDE ORR, JR., WARREN P. HENDRIX
F. KENNETH HURD, and WILLIAM J. CORBETT

DECEMBER 31, 1961

NATIONAL INSTITUTES OF HEALTH
Grant No. S-106

TABLE OF CONTENTS

	Page
I. SUMMARY	1
II. INTRODUCTION.	5
III. EXPERIMENTAL WORK	7
A. Equipment and Operation	7
1. Radial Ion Counter and Associated Electrical Equipment.	7
a. Description	7
b. Operation	12
2. Air Cleaning, Pressure Regulating, and Flow Measuring Equipment	14
3. Aerosol Generating Devices.	16
a. Gasoline Engine	16
(1) Description.	16
(2) Operation.	16
b. DeVilbiss Atomizer.	17
(1) Description.	17
(2) Operation.	17
c. Equipment for Generating Synthetic "Smog"	17
(1) Description.	17
(2) Operation.	19
d. Exploding Wire Device	20
(1) Description	20
(2) Operation	20
e. Benzene-Alcohol Burner for Producing Carbon	21
(1) Description	21
(2) Operation	21

TABLE OF CONTENTS (Continued)

	Page
f. Polymer Aerosol Generator	21
(1) Description	21
(2) Operation	23
4. Equipment for Sharpening the Aerosol Distribution	23
a. Small Ion Remover	23
b. Devices Used to Remove Large Ions	24
5. Aerosol Charging Device	24
6. Devices for Determining the Dew Point of Contaminant Vapors	26
7. Chambers for Controlling Humidities and Aging the Aerosols.	28
8. Miscellaneous Equipment	29
B. Test for the "Affinity" of Various Particle Substances in Organic Vapors.	29
C. Determination of Physical Properties	29
IV. INTERPRETATION OF DATA FROM A RADIAL ION COUNTER	31
V. THEORETICAL PREDICTIONS OF DROPLET GROWTH	43
VI. RESULTS	53
A. Gasoline Exhaust	53
B. Aerosols Produced by Ethanol Solution Atomization	53
C. Paraffin Aerosols.	56
D. Naphthalene Aerosol	56
E. Carbon and Graphite Aerosols	64
F. Poly(Methyl Methacrylate) Aerosol	64
G. Synthetic "Smog".	66

TABLE OF CONTENTS (Continued)

	Page
H. Physical Properties	66
VII. DISCUSSION OF RESULTS	73
VIII. CONCLUSIONS	77
IX. RECOMMENDATIONS.	79
X. APPENDIX.	81
A. References.	83
B. Psychometric Chart for Ethanol in Air	85
C. Tables of Data.	86

This report contains 94 pages.

LIST OF FIGURES

	Page
1. Schematic Diagram of Ion Counter and Related Equipment	8
2. Ion Counter and Related Equipment.	9
3. Ion Counter Detail	10
4. Typical Recording of Voltage Versus Ion Current.	13
5. Aerosol Size Distributions Determined from Electron Micrographs and from Ion Mobility Measurements	15
6. Synthetic Smog Producer.	18
7. Poly(Methyl Methacrylate) Aerosol Generator.	22
8. Ion Generator.	25
9. Water Cooled Dew Point Indicator	27
10. Typical Current Vs. Voltage Curve.	35
11. Experimental Current Vs. Voltage Curve for NaCl.	40
12. Theoretical Growth of 0.025 Micron Radius Camphor Particle with Ethanol Humidity	47
13. Electron Micrograph of Particulate Matter from Gasoline (Unleaded) Engine Exhaust	55
14. Size Distributions Obtained from Ammonium Iodide and Ethanol Systems	62
15. Experimental Growth Curve for 0.02 Micron Radius Poly(Methyl Methacrylate) Particle with Increasing Methyl Ethyl Ketone Relative Humidity	69
16. Comparison of (Poly Methyl Methacrylate) Aerosol Size Distributions Obtained with No Acetone Vapor and in an Atmosphere Very Nearly Saturated with Acetone	70
17. Psychometric Chart for Ethanol in Air.	85

LIST OF TABLES

	Page
I. CALCULATED GROWTH OF AEROSOL PARTICLES WITH INDICATED VAPOR HUMIDITY	48
II. TYPICAL SIZE DISTRIBUTIONS OBTAINED FROM GASOLINE ENGINE EXHAUST	54
III. SIZE DISTRIBUTIONS OBTAINED FOR SYSTEMS OF STEARIC ACID AND ETHANOL	57
IV. SIZE DISTRIBUTIONS OBTAINED FROM SYSTEMS OF CAMPHOR AND ETHANOL.	58
V. SIZE DISTRIBUTIONS OBTAINED FROM SYSTEMS OF AMMONIUM IODIDE AND ETHANOL	59
VI. SIZE DISTRIBUTIONS OBTAINED FROM SYSTEMS OF STEARIC ACID AND TURPENTINE.	60
VII. SIZE DISTRIBUTIONS OBTAINED FROM SYSTEMS OF AMMONIUM IODIDE AND DIOCTYLPHTHALATE.	61
VIII. SIZE DISTRIBUTIONS OBTAINED FROM SYSTEMS OF PARAFFIN AND HEXANE	63
IX. SIZE DISTRIBUTIONS OBTAINED FROM SYSTEMS OF NAPHTHALENE AND GASOLINE	65
X. SIZE DISTRIBUTIONS OBTAINED FROM SYSTEMS OF POLY(METHYL METHACRYLATE) AND METHYL ETHYL KETONE	67
XI. SOLUBILITY DETERMINATIONS.	71
XII. SURFACE TENSION OF SOLUTIONS	72
XIII. CURRENT VERSUS VOLTAGE DATA OBTAINED FOR SYSTEMS OF STEARIC ACID AND ETHANOL	86
XIV. CURRENT VERSUS VOLTAGE DATA OBTAINED FOR SYSTEMS OF CAMPHOR AND ETHANOL.	87
XV. CURRENT VERSUS VOLTAGE DATA OBTAINED FOR SYSTEMS OF AMMONIUM IODIDE AND ETHANOL.	88
XVI. CURRENT VERSUS VOLTAGE DATA OBTAINED FOR SYSTEMS OF STEARIC ACID AND TURPENTINE.	89

LIST OF TABLES (Continued)

	Page
XVII. CURRENT VERSUS VOLTAGE DATA OBTAINED FOR SYSTEMS OF AMMONIUM IODIDE AND DIOCTYLPHTHALATE	90
XVIII. CURRENT VERSUS VOLTAGE DATA OBTAINED FOR SYSTEMS OF PARAFFIN AND HEXANE.	91
XIX. CURRENT VERSUS VOLTAGE DATA OBTAINED FOR SYSTEMS OF NAPHTHALENE AND GASOLINE	92
XX. CURRENT VERSUS VOLTAGE DATA OBTAINED FOR SYSTEMS OF POLY(METHYL METHACRYLATE) AND METHYL ETHYL KETONE.	93

I. SUMMARY

The purpose of this investigation was to determine the physical effect of organic solvent vapors on aerosols having particle radii in the range of 0.01 to 0.1 micron. To accomplish this, an ion counter was employed to determine the particle size distribution of various aerosols both in the presence of pure gases and in the presence of gases containing foreign vapors. The size distributions were established as functions of vapor concentration.

Numerous devices were employed in generating the aerosols. A 2-1/2-horsepower, 4-cycle gasoline engine was used to produce combustion products. Aerosols of soluble materials were prepared by atomization from solvents; stearic acid, camphor, ammonium iodide, paraffin, and naphthalene aerosols were generated in this manner. The solvents were removed from the system by condensation and adsorption. Aerosols of graphite were generated with an "exploding wire" device. A thin film of graphite was deposited on an insulating material and placed between the electrodes of the device in a nitrogen atmosphere. The graphite aerosol was produced upon the instantaneous discharge through the graphite of capacitors totaling 35 microfarads charged to a potential of 10,000 volts. Carbon aerosols were generated with an alcohol-benzene burner. A poly(methyl methacrylate) aerosol was generated by passing a pure nitrogen stream over inhibitor-free methyl methacrylate where it picked up the monomer vapor. The vapor was then irradiated with ultraviolet light to form the polymer aerosol. Finally, synthetic "smog" was produced by irradiating a mixture of nitrogen dioxide, sulfur dioxide, and 1-pentene with ultraviolet light.

Aerosols were brought into contact with a vapor simply by passing the aerosol stream through a container in which a quantity of the vapor substance was

maintained in the liquid state. This liquid's temperature was regulated to ensure its having a certain vapor pressure, and, thus, to provide the desired quantity of vapor. The vapor concentration was checked by dew point measurements in most cases, but in a few instances direct condensation was employed with the condensate quantity being measured.

The distribution of sizes making up the several aerosols was established by measuring the mobility, i.e., the rate of movement in an electric field, of the aerosol particulates carrying an electric charge, i.e., the ions. Since the particulates were limited to radii under 0.1 micron, the maximum charge carried by any one particulate was almost certainly only one electron. This being the case, ion mobilities were readily converted to particulate sizes. The assumption was made that the charged particulates were otherwise no different for having the charge.

Systems consisting of aerosolized particulates (listed first) and a vapor (listed second) such as ammonium iodide and alcohol, camphor and alcohol, poly(methyl methacrylate) and methyl ethyl ketone increased in particulate size with an increase in vapor concentration below relative humidities of 100 per cent, while systems of stearic acid and turpentine, carbon and benzene, graphite and benzene, paraffin and hexane, and naphthalene and gasoline showed no size change below the saturation point. Except for the systems of graphite and benzene and carbon and benzene, the particulates were soluble to a measureable extent in the liquid phase of the vapor with which they were paired.

The process of growth when a nonvolatile particulate is exposed to the vapor of a liquid in which it is soluble is comprised of two distinct mechanisms. The particulate first adsorbs a thin envelope of liquid by physical

attraction of the vapor. This envelope becomes thicker as the relative humidity of the vapor is increased, until, at some particular relative humidity, the particulate dissolves completely. The resulting solution droplet will then continue to grow by the accretion of vapor as the relative humidity is increased. For a given particulate size there is a unique relative humidity at which total dissolution will occur, and this relative humidity can be calculated using data on the surface energy of the solid and the surface tension and vapor pressure of the resulting solution. After the soluble particulate has become a solution droplet, its size upon exposure to any higher relative humidity can be calculated from a knowledge of the vapor pressure of the solvent and the vapor pressure and surface tension of the solution. In general, theory predicts that the higher the solubility of the particulate in the solvent to which it is exposed the lower will be the relative humidity at which a solution droplet will form. For very small particulate diameters (on the order of hundredths of a micron) of relatively low solubility materials (less than approximately 5 per cent by weight) the theory predicts that a solution droplet will not form until the relative humidity exceeds 100 per cent.

The experimental results of this investigation are in agreement with these predictions.

II. INTRODUCTION

Hygroscopic particles in the atmosphere pick up or lose water vapor if the ambient humidity changes. As a result they shift from discrete solids through supersaturated and saturated droplets to dilute solution droplets and back again. Each step is accompanied by a change in particulate size. This behavior has been described in considerable detail.^{1,2,3,4*} Dioctylphthalate (DOP) droplets, in addition, have been shown to increase in size when exposed to toluene vapor and to do so in accordance with the Kelvin equation, at least to sizes as small as 0.03 micron in radius.^{5,6} Other particulates would also be expected to take up organic vapors if brought into contact with them. Since the association of vapors and airborne particulates may have considerable influence on the course of air pollution,⁷ this presentation covers the change in size of various particulates from 0.01 to 0.10 micron in radius upon exposure to several organic vapors.

*References are tabulated in the Appendix.

III. EXPERIMENTAL WORK

A. Equipment and Operation

Essentially, the apparatus used in this investigation consisted of (1) a radial ion counter with its associated electrical equipment, (2) air cleaning, pressure regulating, and flow measuring devices, (3) aerosol generating systems, (4) devices for sharpening the aerosol size distributions, (5) an aerosol charging device, (6) instruments for determining the concentration of contaminant vapors, (7) chambers for controlling the vapor humidities and for aging the aerosols, and (8) miscellaneous equipment for preparing and analyzing aerosol distributions. A schematic diagram of the apparatus is shown in Figure 1.

1. Radial Ion Counter and Associated Electrical Equipment

a. Description. A cylindrical ion counter was previously used by these investigators^{5,8} to measure the increase in size of hygroscopic nuclei as a function of relative humidity. For this investigation a similar device was selected. A radial design was chosen because of the ease with which such a counter could be disassembled, cleaned, and realigned. Some difficulty was encountered during construction due to the necessity for machining quite flat circular electrodes. To do this, stainless steel plates were annealed to relieve stresses and faced on a lathe. After several facings, taking very small cuts, the plates were within approximately three-thousandths of an inch of being flat, and calculations were made to determine the possible error due to this uncertainty. The error introduced was found to be negligible for the purposes of this investigation.

The radial ion counter with its associated electrical equipment is shown in Figure 2. Figure 3 is an engineering drawing of the ion counter which

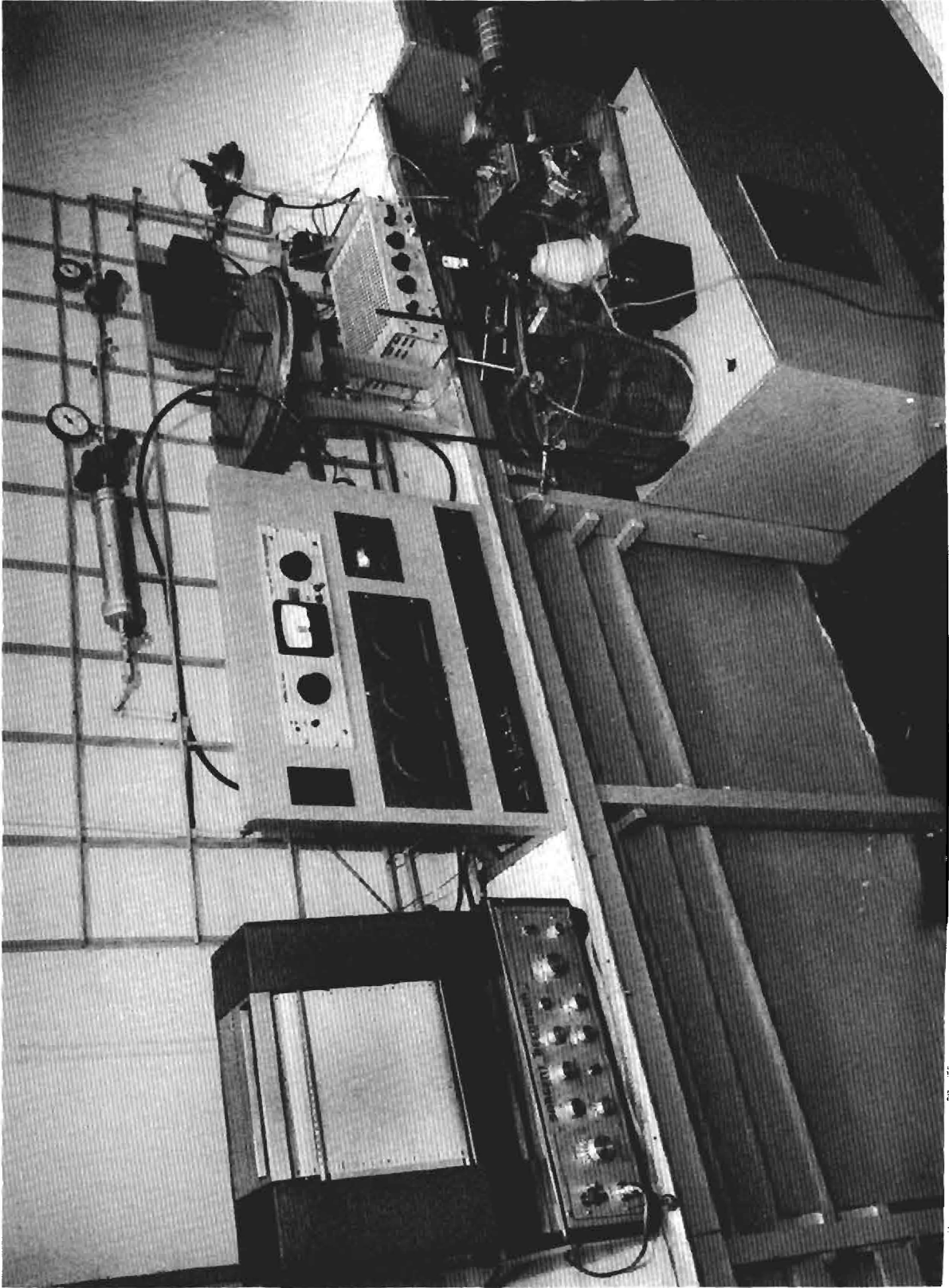


Figure 2. Ion Counter and Related Equipment.

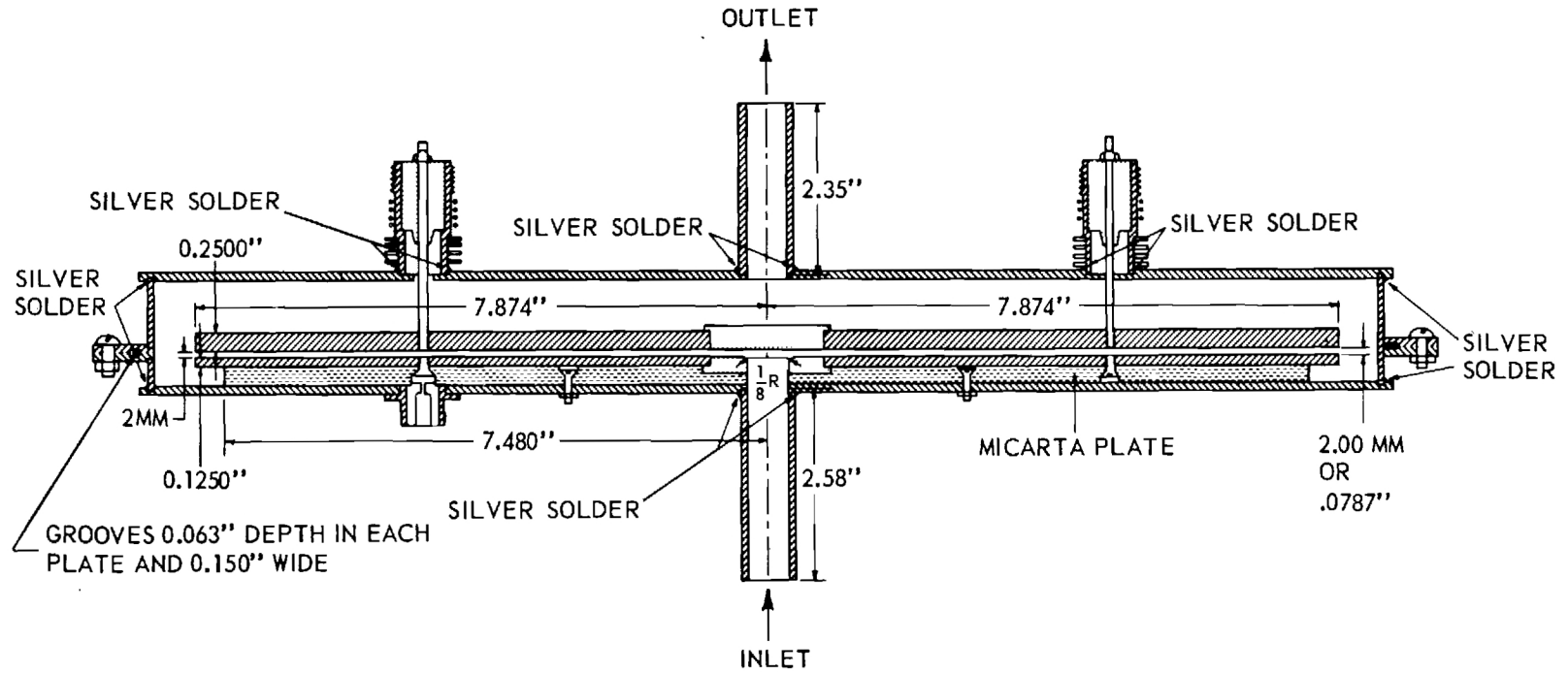


Figure 3. Ion Counter Detail.

basically consists of two circular, stainless steel electrodes 40 centimeters in diameter with a 4-centimeter-diameter center section removed from each and both enclosed in a grounded electrostatic shield. The top electrode was suspended from the electrostatic shield by four stainless steel rods inserted through cylindrical Teflon insulators mounted above the shield. The Teflon insulators were heated approximately 5°C above the other parts of the counter to prevent condensation on the Teflon. The heaters were wound from resistance wire connected in series. Approximately 10 volts A.C. were applied across the heaters from a variable voltage transformer. Cooling fins were provided on the insulator holders between the heaters and the counter to prevent the heaters from disturbing the temperature maintained in the ion chamber. The bottom electrode was mechanically attached to the electrostatic shield, but it was electrically insulated from it by a 1/4-inch-thick Teflon sheet. Four-centimeter-diameter Teflon discs were press-fit in the center of each electrode to insure that laminar flow was fully developed before reaching the active portion of the electrodes. An aerosol entrance port of one centimeter was provided in the center of the bottom electrode.

The distance between the electrodes was adjusted by raising the top electrode, initially at rest on the bottom electrode, to the desired distance. At first this distance was measured with an optical micrometer by observing the stainless steel supports protruding through the electrostatic shield. This technique was discarded in favor of a partially cutaway cap with an adjustment screw in the top. The distance between the adjustment screws and the stainless steel supports was set using a spacer of the proper thickness with the top electrode at rest on the bottom electrode. The top electrode was then raised until all supports came into contact with the

adjusting screws. The top electrode was electrically connected to ground through a micro-microammeter, Model 410, manufactured by Keithley Instruments, Inc., Cleveland 6, Ohio. The bottom electrode was connected to a Keithley, Model 240, regulated variable high voltage supply which provided voltages from 0 to 1000 in 1/10-volt increments with an accuracy of plus or minus one per cent or 1/10 of a volt. All connectors were shielded Teflon-insulated cables.

The ground electrostatic shield surrounding the two electrodes was constructed of 1/8-inch stainless steel sheet and was designed to permit ready access for cleaning of the electrodes. The aerosol entered through the bottom of the shield, passed radially outward between the electrodes and was exhausted through an opening in the top of the shield. The reading of the micro-microammeter was monitored with a recorder, Type S-72150, manufactured by E. H. Sargent and Company, Chicago 30, Illinois.

b. Operation. The electrical power to the micro-microammeter, recorder, and variable voltage supply was turned on and each instrument was allowed to equilibrate before determinations were attempted. The recorder was standardized and the recorder and the micro-microammeter were set at zero according to instrument instructions. An aerosol, from the appropriate generating device, was passed through the various conditioning parts of the system at the desired flow rate into the ion counter. The voltage applied to the bottom plate was increased periodically by known increments, and the current resulting from the migration of ions to the top electrode was indicated by the micro-ammeter and recorded. A typical recording of the ion current at the various voltages is shown in Figure 4. The chart speed is one inch per minute for this recording. Either positive or negative

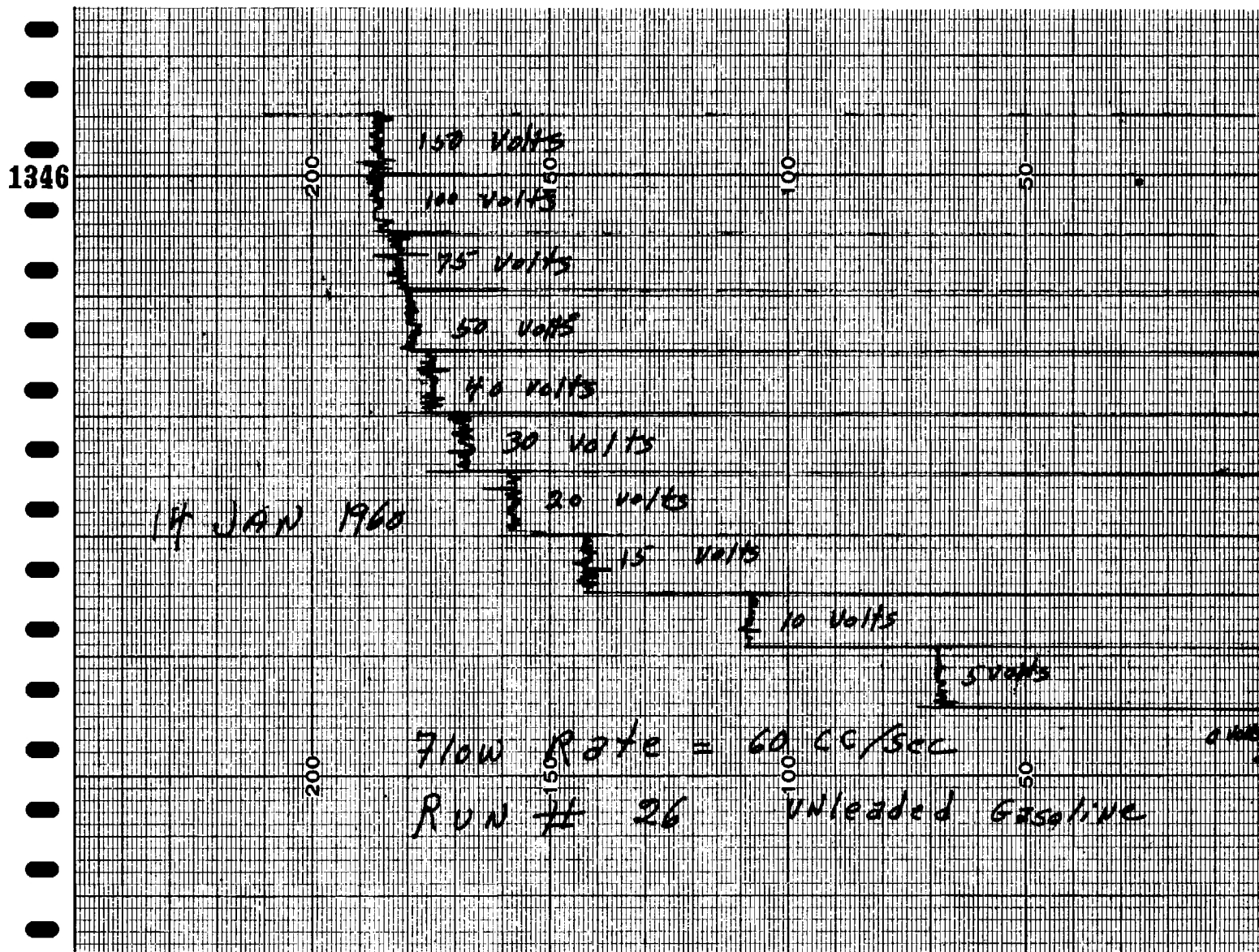


Figure 4. Typical Recording of Voltage Versus Ion Current.

ions could be measured by reversing the polarity of the applied voltage and reversing the scale directions on both the micro-microammeter and the recorder.

To determine if a change in the size distribution of an aerosol occurred one method was to set the applied voltage so that only a portion of the ions were removed and then to increase or decrease the relative humidity of the contaminant vapor. If an increase in particle size occurred, decreasing the mobility, fewer particles would be collected at the particular applied voltage and a decrease in ion current would be noted. A second method was also employed. For some aerosols such as carbon and graphite, two identical humidity chambers were constructed, one containing a very high relative humidity of the contaminant and the other containing a very low relative humidity. The aerosol stream would be diverted through first one chamber and then the other with a large stopcock. This is the quickest method for determining if a change in particle size does occur; however, absolute values cannot be deduced from the method. The concentration of the contaminant vapor was measured on the exhaust side of the ion counter. The method of obtaining a size distribution from the ion current versus voltage recording is described in detail in Section IV.

To assure that the ion counter was operating properly the size distribution obtained with the ion counter for an aerosol resulting from atomizing a dilute solution of sodium chloride was compared with the distribution obtained from electron micrographs of the same aerosol. Such a comparison is shown in Figure 5.

2. Air Cleaning, Pressure Regulating, and Flow Measuring Equipment

Air was taken directly from a compressed air line at approximately 90 pounds per square inch and reduced to 20 pounds per square inch with a pressure regulator. The air passed from the pressure regulator to a surge tank

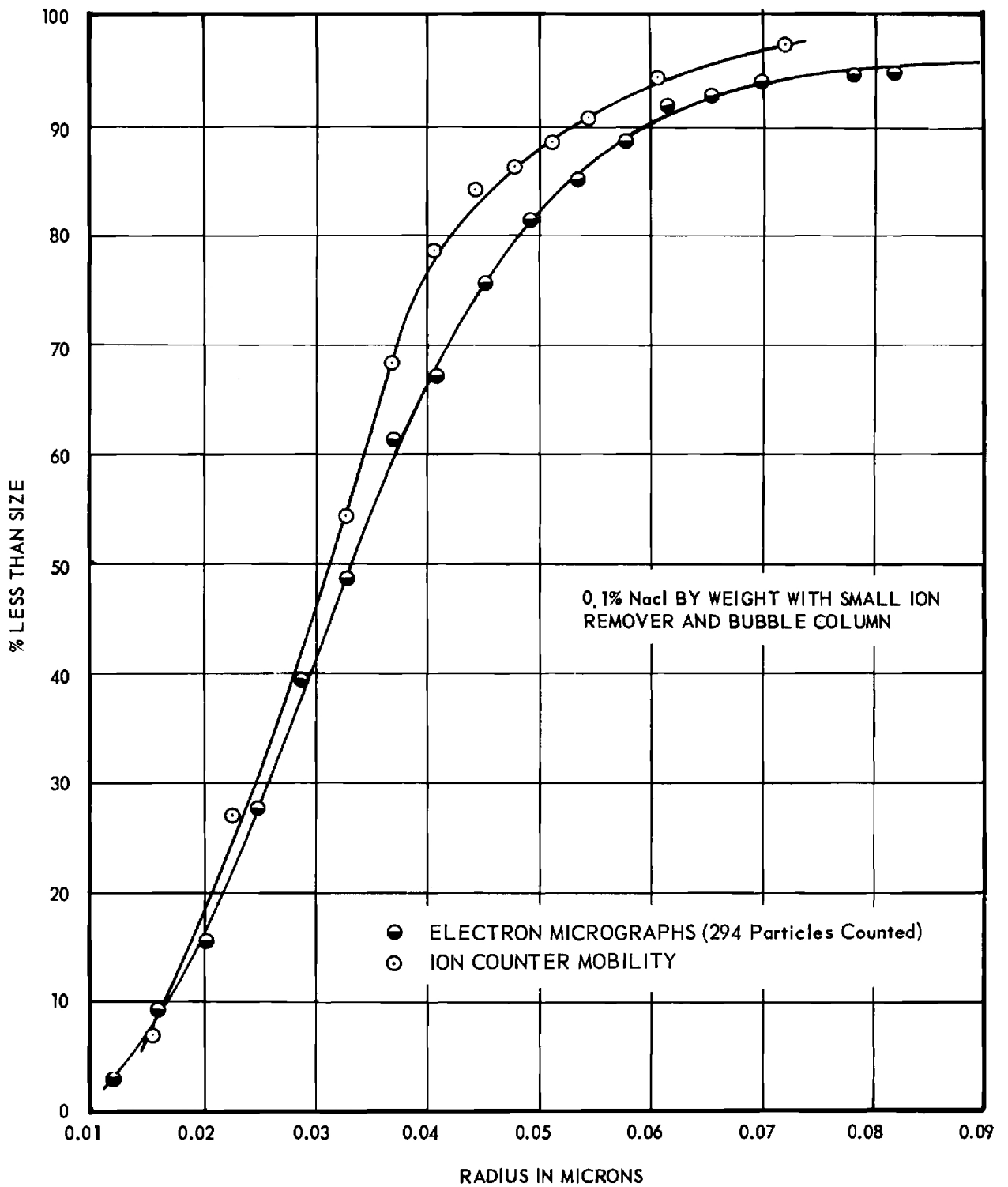


Figure 5. Aerosol Size Distributions Determined from Electron Micrographs and for Ion Mobility Measurements.

and filter, then to a second pressure regulator where the pressure was reduced to the desired level. Rotometers were used to measure the rates of flow throughout the system. In systems where low flow rates were desired for introducing gases, stainless steel metering valves, manufactured by Nuclear Products Company, Cleveland 10, Ohio, were used. In systems requiring the aerosols to be charged, the excessive air required for proper operation of the charging device was bled from the line before it entered the main portion of the system.

3. Aerosol Generating Devices

a. Gasoline Engine

(1) Description. A 4-cycle engine, Model 6012, manufactured by the Briggs and Stratton Corporation, Milwaukee 1, Wisconsin, equipped with a glass-wool packed muffler, was used to produce gasoline engine exhaust. Since the exhaust from the engine was too great and too pulsating for direct ion counter analysis, an aspirator was employed to withdraw a continuous sample from the exhaust stream.

(2) Operation. The gasoline engine was filled with the desired type of gasoline, started, and allowed to run for several minutes so that maximum stability could be attained. A portion of the exhaust gas was pulled into a large air stream by means of the gas aspirator. The aerosol was then passed through chambers of regulated temperature to adjust the aerosol to a predetermined humidity and to establish the humidity history of the aerosol. The aerosol then passed into a large aging chamber where it was irradiated with ultraviolet light. The average time in the irradiation chamber was determined from the flow rate. After irradiating, the aerosol passed to the ion counter.

b. DeVilbiss Atomizer

(1) Description. Aerosols from soluble material were generated from dilute solutions by atomization, utilizing a DeVilbiss No. 180 atomizer, manufactured by the DeVilbiss Co., Toledo, Ohio. The atomizer produces fairly uniform droplets of approximately one micron diameter when operated with a sufficient forepressure.

(2) Operation. The aerosol material was dissolved in an organic solvent. The atomizer was then filled with a solution containing the desired concentration of the material from which the aerosol was to be generated and connected to an air line with a pressure of approximately 13 pounds per square inch. The aerosol stream was heated immediately after atomization to lower the relative humidity of the solvent vapor and to ensure that solid particles of the aerosol were formed. The solvent was removed from the system by adsorption or freeze-out techniques. The aerosol was then passed through the conditioning chambers to the ion counter.

c. Equipment for Generating Synthetic "Smog"

(1) Description. The equipment necessary to generate smog synthetically⁹ is shown in Figure 6. It consisted of a small chamber containing two Teflon bags for storing the required gases, two stainless steel metering valves, two glass rotometers, a Teflon-lined chamber for irradiating the gases after mixing, an ultraviolet irradiation source, and a device for inducing an electrical charge on the resulting aerosol.

The irradiation chamber was a cylindrical drum 32 inches high by 24 inches in diameter and lined with Teflon. The chamber contained an irradiation source consisting of four ultraviolet lamps with a total rating of

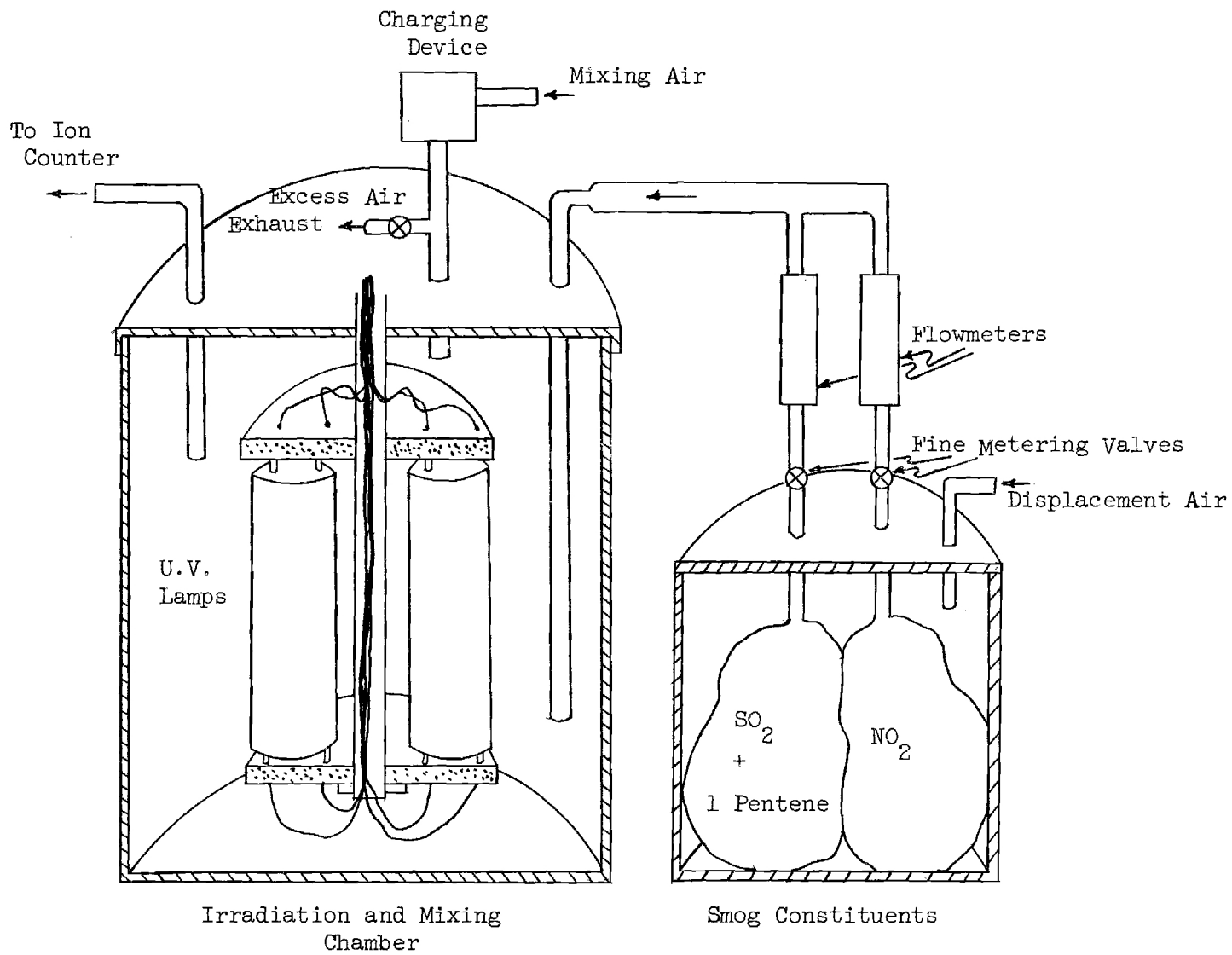


Figure 6. Synthetic Smog Producer

60 watts. The ballasts and starters were mounted on the outside of the chamber to prevent reactions with the contaminated atmospheres produced in the chamber. A charging device, described in a following section, was mounted on top of the chamber to induce an electrical charge on the resulting aerosol particulates.

(2) Operation. Air was forced into the part of the smaller chamber not containing the Teflon bags, until the air and gases in the bags were exhausted. A known quantity of nitrogen dioxide was placed in one bag and known quantities of sulfur dioxide and 1-pentene were placed in the other. The bags were then completely filled with known quantities of air metered with a wet test meter at atmospheric pressure. Again air was forced into the outer part of the chamber, but this time it caused the gases to flow through the stainless steel metering valves, the rotometers, and into the irradiation chamber. The desired flow was attained by adjusting the valves. The ultraviolet lamps were turned on and the air flow to the charging device was started. Since the air rate necessary to operate the charging device was greater than desired through the chamber, only a portion of it was allowed to enter the irradiation chamber where it was mixed with the incoming gases. The average time of irradiation in the chamber was controlled by the flow rates.

The aerosol produced after a few minutes by irradiation was passed through the conditioning chambers to the ion counter.

d. Exploding Wire Device

(1) Description. An exploding wire device¹⁰ was used for generating aerosols such as graphite for ion counter analysis. The unit was essentially a 35-microfarad capacitance bank, a power supply capable of charging these capacitors to 10,000 volts, an explosion chamber with sample holders and a switching mechanism to discharge the capacitors across the sample. The explosion chamber was constructed of 1/8-inch stainless steel with a transparent door for loading and observing the sample. In addition, a port was provided in each end of the chamber so that it could be filled with an inert atmosphere or maintained at reduced pressures. The sudden release of electrical energy provides the heat of vaporization and the explosive force necessary to generate an aerosol.

(2) Operation. Graphite powder to be aerosolized was placed on a cutaway piece of Tygon tubing with copper rods in each end. The graphite was wet with water to make it more conducting and spread evenly between the copper rods. The copper rods were then connected to the electrical contacts in the explosion chamber, and the explosion chamber was filled with a nitrogen atmosphere. The capacitors were charged to approximately 10,000 volts and then discharged suddenly through the graphite breaking up and dispersing it. The explosion chamber was next connected to the outside portion of a larger chamber containing a bag filled with air. The graphite aerosol was pulled into the chamber by withdrawing the air from the bag with a water aspirator. The chamber containing the aerosol was then stirred with a fan to insure uniform mixing, and finally, was connected to the ion counter system. The aerosol was forced through the counter by

refilling the bag with air. This batch type system was selected in order to prevent the aerosol from being diluted with air after it had been prepared.

e. Benzene-Alcohol Burner for Producing Carbon

(1) Description. The burner employed in producing an aerosol of carbon consisted of a small container with a wick across which was blown a jet of nitrogen gas to prevent complete combustion and aerosol agglomeration.

(2) Operation. When the burner was lighted and the nitrogen jet was adjusted to prevent complete combustion, a portion of the resulting aerosol was sucked into an air stream with a gas type aspirator. The diluted aerosol then passed through a mixing chamber and through various other conditioning chambers to the ion counter.

f. Polymer Aerosol Generator

(1) Description. A schematic diagram of the apparatus for generating poly(methyl methacrylate) aerosol¹¹ is shown in Figure 7. It consisted of a pressure regulated nitrogen gas supply, a chamber containing copper turnings inside a muffle furnace to remove all the oxygen that might be in the nitrogen stream, a chamber for introducing the monomer, and the polymerization chamber. A circular quartz window approximately 2 inches in diameter was located in the polymerization chamber to permit the passage of ultraviolet light. The ultraviolet light source was a quartz mercury arc lamp of the Central Scientific Company, Chicago, Illinois. This light directed through the quartz window activated the monomer causing small nuclei of polymer to form on which the remaining monomer could react. The result was an aerosol of poly(methyl methacrylate).

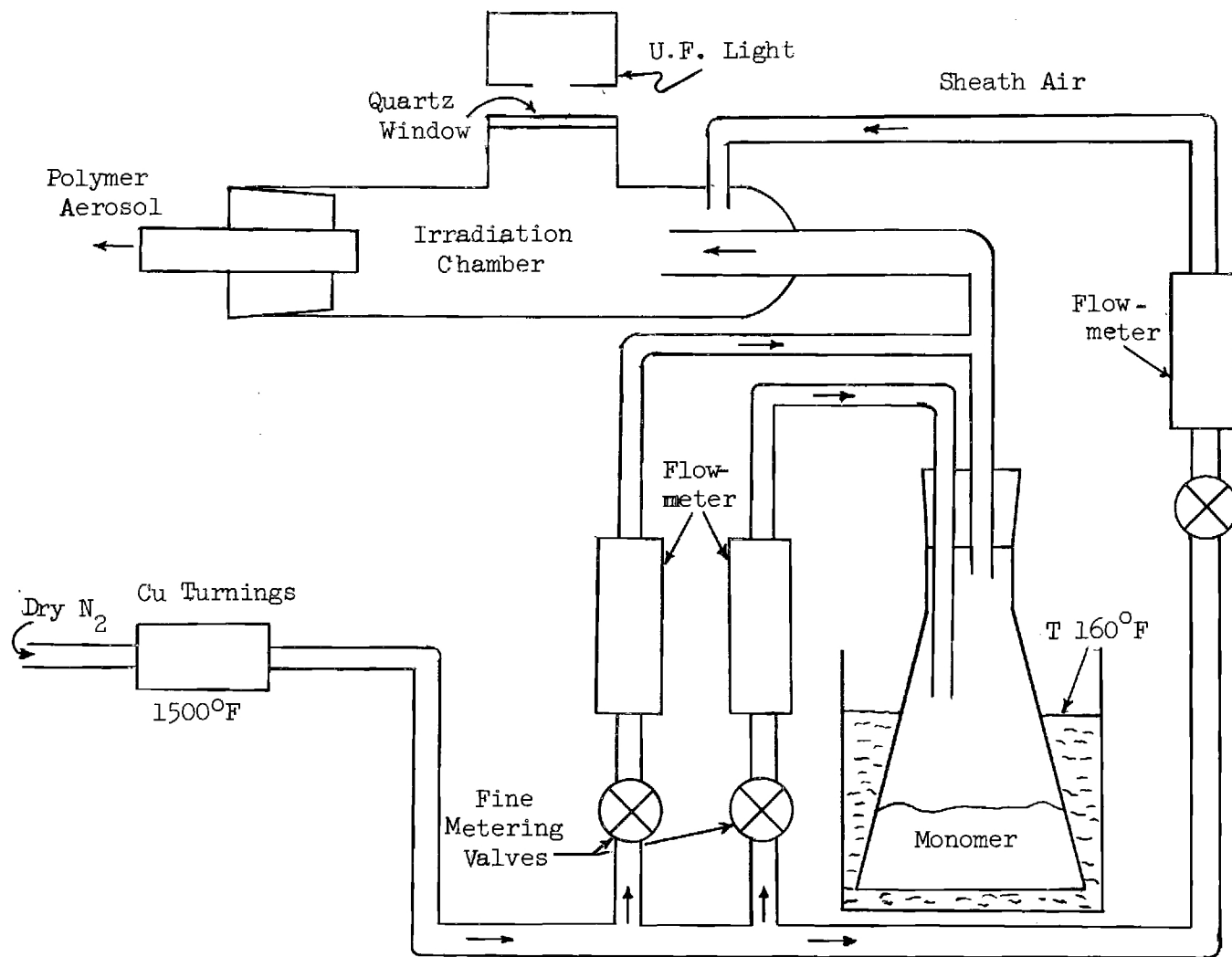


Figure 7. Poly(Methyl Methacrylate) Aerosol Generator

(2) Operation. Approximately 30 milliliters of methyl methacrylate monomer were treated with 25 milliliters of 5 per cent sodium hydroxide solution to remove the inhibitor. After thoroughly mixing and allowing sufficient time for reaction with the inhibitor, the aqueous phase (bottom layer) was removed using a separatory funnel. The methyl methacrylate which remained was washed several times with water until a negative reaction for the OH^- was indicated upon a litmus paper test. Molecular sieve of the Linde Air Products New York 17, New York, was then used to dry the inhibitor-free monomer, and a portion of it was placed in the monomer container shown in Figure 7. The bottom of the container was placed in a water bath which was maintained at 160°F . A known quantity of the oxygen free nitrogen was next passed through the monomer container where it picked up the monomer vapor. The vapor passed into the polymerization chamber at a linear velocity of 0.5 cm/sec. The sheath stream flow rate was 774 cc/min which gave it the same flow velocity as the monomer. The ultraviolet light was directed through the quartz window into the polymerization chamber, catalyzing the polymerization and causing the poly(methyl methacrylate) aerosol to form. The aerosol, finally, was passed through the desired conditioning chambers to the ion chamber.

4. Equipment for Sharpening the Aerosol Distribution

In certain systems, sharpening, i.e., making more nearly monodisperse, the aerosol distribution was deemed desirable. This was accomplished by removing both the smaller and larger ions with devices as indicated below.

a. Small Ion Remover

The small ion remover was a miniature stainless steel radial ion counter designed to remove all charged particles with a radius of less

than 0.005 micron. It permitted a gas flow of 60 cc/sec and had a plate separation of 3 millimeters. The top electrode was grounded directly and a positive potential was connected to the bottom electrode. This device removed all charged particles of the designed radius and a portion of the larger sizes which happened to enter near the collecting electrode. The remaining particles were sufficient in number for size distribution tests and determinations. Therefore, no attempt was made to measure the portion of the total number of particles extracted.

b. Devices Used to Remove Large Ions

Two types of media have been used to remove ions larger than about 0.1 micron in radius. The first was a 3-1/2-inch column filled to a depth of 30 inches with water. The gas stream containing the aerosol was introduced at the bottom of this column through a wire mesh which broke the stream in small bubbles. The second remover was a filter of glass wool placed directly in the gas stream immediately following the aerosol generator.

5. Aerosol Charging Device

An ion generator of the type developed by Whitby, et al.,¹² was used to charge the particulates of several of the aerosols investigated which normally were only partially charged. The device consisted of a direct current, high voltage supply variable from 0 to 10,000 volts constructed especially for the purpose, and a device for inducing the electric charge as shown in Figure 8. The actual charging device consisted essentially of a cylindrical Plexiglas chamber with sealed ends and two stainless steel electrodes. One electrode was in the form of a thin disk with a 1/16-inch-diameter hole through its center. The other electrode was a pointed rod.

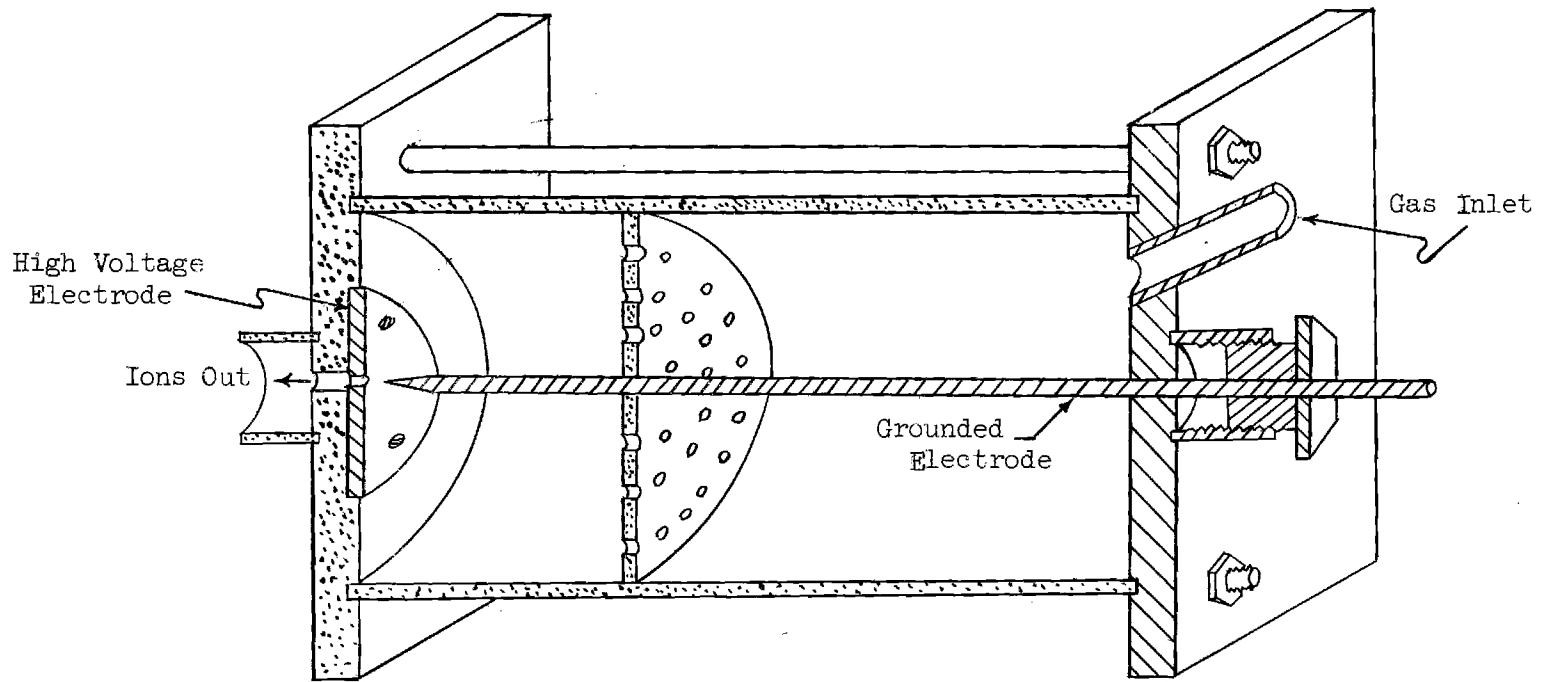


Figure 8. Ion Generator

In use the point was centered above the hole in the disk at a distance determined by gas flow and voltage requirements. The rod was maintained at ground potential. Air, or other gas was fed into the chamber at a pressure of 15 pounds per square inch; it exhausted through the electrode with the center hole. A corona discharge was established between the electrodes, and the passing gas carried the charges outside the unit where they could be mixed with aerosol particulates. An aerosol could be charged either positive or negative depending on the polarity of the electrodes.

6. Devices for Determining the Dew Point of Contaminant Vapors

The dew point of contaminant vapor was determined by measuring the temperature at which they condensed on a mirrored surface. Figure 9 shows schematically one apparatus which utilized water to cool a small brass sheet, approximately 1/32-inch thick, with a polished chrome finish on one side. The temperature of the water was controlled by mixing a stream of water that had passed through a cold bath with a stream of water at approximately room temperature. Using a mixture of ice and salt in the cold bath, temperatures to approximately 5°C were readily obtained. The temperature of the brass sheet was considered to be that of the water stream, and the latter was measured with Bureau of Standards thermometers, calibrated in 1/10-degree increments, before and after the test section. Condensation was indicated by directing a beam of light at the polished surface and measuring the reflected light picked up by a cadmium sulfide photocell. The photocell was incorporated as one leg of a null bridge circuit which was balanced when there was no condensation on the polished surface. The unbalance from condensation was indicated by a galvanometer, Model 440, manufactured by Western Electric

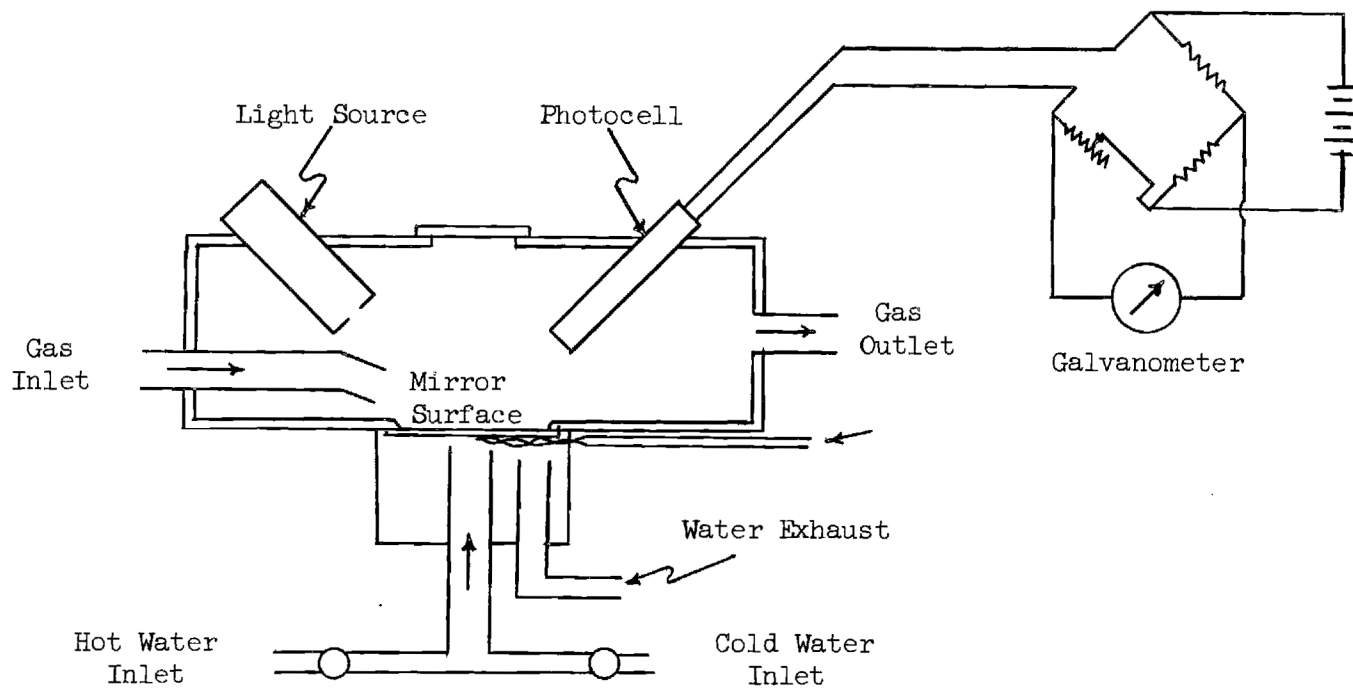


Figure 9. Water-Cooled Dew Point Indicator

Instrument Corporation, Newark, New Jersey. This design was slightly troublesome to operate; however, it was quite accurate in the hands of an experienced operator.

A second design operating on the same principle was constructed for continuous monitoring of the dew point. A cadmium sulfide photocell was employed as the detector; it served as one arm of a 60-cycle A.C. null bridge. The photocell operated a relay which controlled the power supply of a Frigistor, Model FS4, manufactured by the General Thermoelectric Company, Princeton, New Jersey. The Frigistor maintained a brass plate 1/32-inch thick with a mirrored chrome finish on one side and approximately the same area as the Frigistor (1/2 by 3/4 inch), at the temperature of the dew point. The excess heat from the Frigistor was dissipated by circulating water. The dew point temperature was measured with a calibrated thermocouple attached to the plate. The e.m.f. from the thermocouple was amplified with a stabilized direct current microvolt amplifier, Model 9835D, manufactured by the Leeds and Northrup Co., Philadelphia, 44, Pennsylvania, and monitored with a recorder Model SR, manufactured by E.H. Sargent & Co., 4647 W. Foster Ave., Chicago 30, Illinois. This device is only semiautomatic in that the current to the Frigistor must be adjusted manually for different dew point temperature ranges.

7. Chambers for Controlling Humidities and Aging the Aerosols

The chambers used to control the humidity of the various contaminants were 2-liter glass flasks mounted in temperature-controlled water baths; material for adding vapor to or adsorbing vapor from the system was contained in the flasks also. The aging chamber varied from a 300-liter box to a one-liter boiling flask depending on the system being investigated; in

some instances no aging chamber was used.

8. Miscellaneous Equipment

An electron microscope was used to make micrographs from which particle sizes were then determined. Optical microscopes with an optical micrometer were used to analyze the electron micrographs. A thermal precipitator was employed to collect samples on the electron microscope grids. A Traube stalagmometer was used to measure the surface tension of the various solutions, while their densities were measured with a pycnometer.

B. Test for the "Affinity" of Various Particle Substances in Organic Vapors

Tests were made to determine if certain of the aerosol substances adsorbed enough contaminant solvent vapor from a saturated atmosphere to dissolve partially or completely. To do this the dessicant space of a large dessicator was filled with one of several organic solvents. A few particles of the different aerosol materials were then placed on microscope slides and enclosed in the container with the solvent. The particles and vapor were allowed to equilibrate overnight, after which, visual observations were made to see if swelling, dissolution, or partial dissolution of the particles had occurred. These determinations were used to see if aerosol growth in the presence of vapor might be expected. No absolute conclusions were drawn from these observations, but they were found to be a general guide to an aerosol's behavior.

C. Determination of Physical Properties

Solubility and surface tension data were needed for theoretical calculations of the systems investigated. In many cases such data could not be found in the literature and had to be determined experimentally.

To establish solubilities, a 100-gm sample of solvent, which had been

brought to 25°C in a temperature-controlled bath, was placed into a thoroughly cleaned, dried, and weighed Erlenmeyer flask. A flask of dry solute was also prepared and weighed. The solute was next added slowly to the solvent until a small amount remained undissolved. The flask was then placed in a controlled temperature bath at 25°C and allowed to remain for several days with occasional agitation. Additional solute was added as the previous amount dissolved. After the final equilibrium, the flask containing the solvent and the solute and the flask containing the solute were reweighed. From the differences, solubilities were calculated as was the evaporation of solvent during the test. This latter proved to be a negligible quantity in all systems.

Surface tension determinations were made with a Traube stalagmometer. The procedure, briefly, was to clean the equipment with cleaning solutions and rinse it with distilled water. The stalagmometer was then filled with the solvent, and subsequently, with the solvent containing various concentrations of the solute. The size and number of the drop emerging were determined at 25°C. A pycnometer was used to determine the densities of the pure solvent and solvent with various weight per cents of contained solutes when these data could not be obtained from the literature. The surface tension σ was calculated from the equation

$$\sigma = \frac{\sigma_w N_w \rho}{N \rho_w} \quad (1)$$

where σ_w is the surface tension of water, N is the number of sample drops, N_w is the comparative number of pure water drops obtained with the stalagmometer, ρ is the density of the sample, and ρ_w is the density of water.

IV. INTERPRETATION OF DATA FROM A RADIAL ION COUNTER

For laminar flow between the circular plates of the ion counter, the velocity profile of the air flow in cylindrical coordinates is

$$v_R = \frac{b^2 \Delta P}{2R\mu \ln \frac{R_2}{R_1}} \left[1 - \left(\frac{z}{b}\right)^2 \right] \quad (2)$$

where v_R is the radial velocity, R is the distance from the center of the circular plates, b is the distance between the two plates, R_1 is the inner radius, R_2 is the outer radius, ΔP is the pressure drop from the inner radius to the outer radius, μ is the viscosity of the air, and z is the displacement along the vertical axis with the origin midway between the plates.

Since the flow rate, F , can be expressed as

$$F = \int_{-b}^{+b} v_R (2\pi R) dz \quad (3)$$

integration yields

$$F = \frac{4}{3} \left[\frac{\pi b^3 \Delta P}{\mu \ln \frac{R_2}{R_1}} \right] \quad (4)$$

Equation 4 may then be substituted into Eq. 2 to give the velocity profile as a function of F , z , and R . The resulting equation is

$$v_R = \frac{3F}{8b \pi R} \left[1 - \left(\frac{z}{b}\right)^2 \right] \quad (5)$$

The mobility of a charged particle in an electric field is defined as the velocity per unit field strength. If a distribution of ions with a single discrete mobility, ω_i , is considered

$$\omega_i = \frac{v_z}{E} \quad (6)$$

where v_z is the velocity in the z direction and E is the field strength.

The field strength between the parallel plates is

$$E = \frac{V}{2b} \quad (7)$$

where V is the applied potential difference between the plates. Substituting Eq. 7 into Eq. 6 the mobility of each ion is

$$\omega_i = \frac{2bv_z}{V} \quad (8)$$

The z coordinate of an ion with mobility ω_i entering the chamber at R_1 and Z_0 is given at time, t, after entering as

$$z = Z_0 + v_z t \quad (9)$$

Substituting this relation into Eq. 5 yields

$$v_R = \frac{dR}{dt} = \frac{3F}{8b\pi R} \left[1 - \left(\frac{Z_0 + v_z t}{b} \right)^2 \right] \quad (10)$$

A particle initially at Z_0 will reach the lower plate and be collected at a time t_f given by

$$t_f = \frac{b - Z_0}{v_z} \quad (11)$$

Integration of Eq. 9 and substitution of Eq. 11 into Eq. 10 results in

$$\frac{R_c^2 - R_1^2}{2} = \frac{F}{8b\pi v_z} \left[\frac{z_o^3}{b^2} + 2b - 3z_o \right] \quad (12)$$

The above equation gives them R_c at which an ion initially at Z_o will be collected. By setting R_c equal to R_2 the equation may be rearranged to give

$$v_z = \frac{F}{4b^3\pi} \left[\frac{z_o^3 - 3b^2z_o + 2b^3}{R_2^2 - R_1^2} \right] \quad (13)$$

and substitution of v_z from Eq. 8 gives

$$V = \frac{F[z_o^3 - 3b^2z_o + 2b^3]}{2\pi b^2\omega_i [R_2^2 - R_1^2]} \quad (14)$$

The above equation gives the minimum voltage, V , required to collect an ion of mobility ω_i entering the chamber at Z_o . All ions with $z > Z_o$ will also be collected. The number of ions entering the chamber at R_1 with $z > Z_o$ is

$$N = 2\pi R_1 n_i \int_{z_o}^{+b} v_r dz \quad (15)$$

where n_i is the number of ions of mobility ω_i per cubic centimeter

Integration of Eq. 15 yields

$$N = \frac{n_i F}{4b^3} [2b^3 - 3b^2z_o + z_o^3] \quad (16)$$

In order to obtain the number of ions collected per second as a function of voltage, Eq. 16 and Eq. 14 may be combined to eliminate Z_0 , yielding the important result that

$$N = V \omega_i n_i \pi \left[\frac{R_2^2 - R_1^2}{2b} \right] \quad (17)$$

which means that for a discrete mobility the number of ions collected is a linear function of the applied voltage until, of course, all the ions are collected.

The preceding equations, although derived for a single mobility ω_i , are valid for each mobility in a mobility distribution.

Before proceeding further, it is necessary to know what fraction of the ions of mobility ω_i will be collected for a specific applied voltage V_0 . The specific voltage V_0 chosen is that voltage which will just collect all the ions of mobility, ω_0 . Thus Eq. 14 with $Z_0 = -b$ becomes

$$V_0 = \frac{2Fb}{\omega_0 \pi (R_2^2 - R_1^2)} \quad (18)$$

If V_0 from Eq. 18 is inserted for V in Eq. 17

$$N = Fn_i \frac{\omega_i}{\omega_0} \quad \text{or} \quad \frac{N}{Fn_i} = \frac{\omega_i}{\omega_0} \quad (19)$$

But Fn_i is the total number of ions of mobility ω_i which are entering the ion counter. Thus for $\omega_i < \omega_0$, ω_i/ω_0 is the fraction of the ions of mobility ω_i which will be collected at a voltage V_0 .

A typical ion-current versus voltage curve is shown in Fig. 10. Under

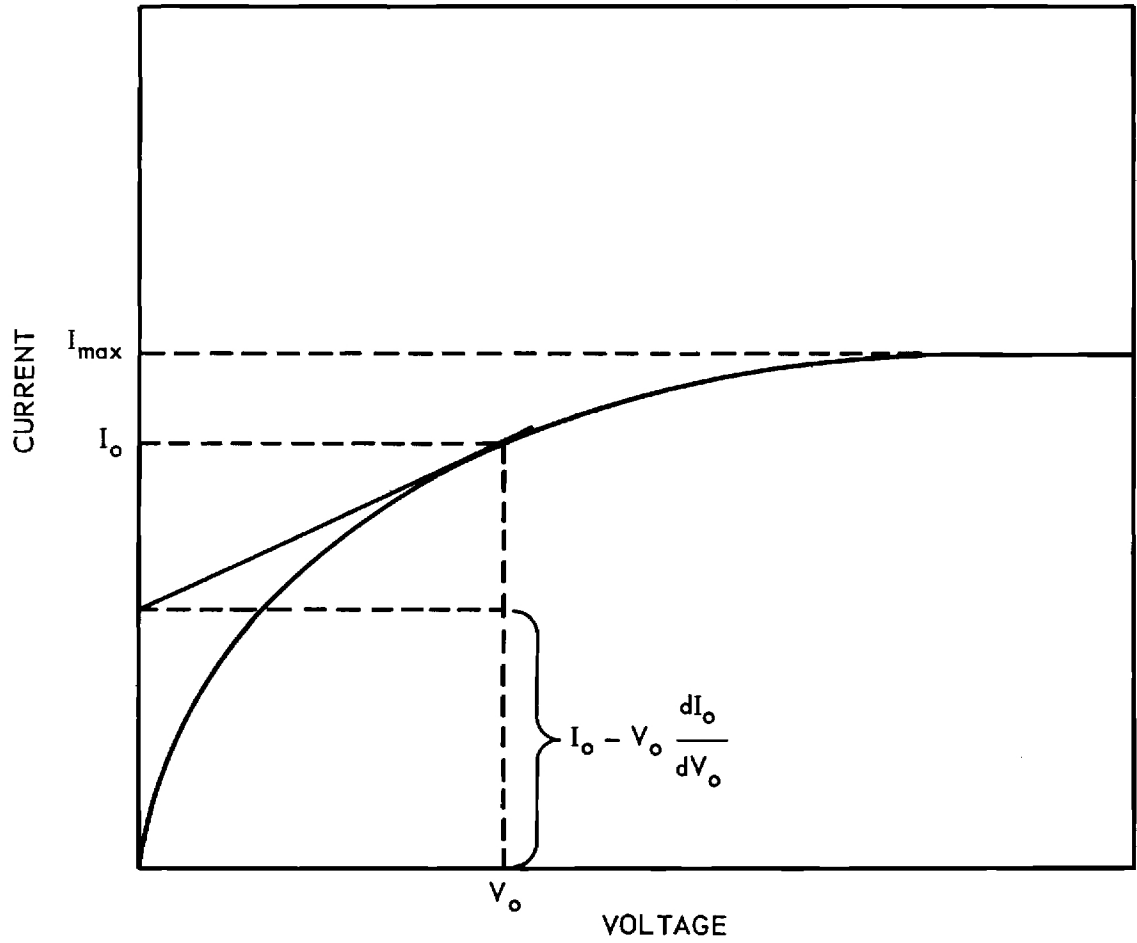


Figure 10. Typical Current Vs. Voltage Curve.

the assumption than an ion carries only one electronic charge the curves may be interpreted in terms of mobility and size distribution.

For a continuous ion mobility distribution the frequency $f(\omega)$ is defined by

$$\int_0^{\infty} f(\omega) d\omega = 1 \quad (20)$$

The relationship between $f(\omega)$ and the current-voltage curve must next be established and finally related to ion size. For the specified voltage V_0 all ions of mobility $\omega \geq \omega_0$ are collected and produce a current

$$I_1 = I_{\max} \int_0^{\infty} f(\omega) d\omega \quad (21)$$

where I_{\max} is the current obtained when the entire distribution is collected. For ions of mobility $\omega < \omega_0$ the fraction ω/ω_0 of the ions of mobility ω which is collected produces a current

$$I_2 = \frac{I_{\max}}{\omega_0} \int_0^{\omega_0} \omega f(\omega) d\omega \quad (22)$$

Thus the total current I_0 corresponding to an applied voltage V_0 is given by

$$I_0 = I_{\max} \frac{1}{\omega_0} \int_0^{\omega_0} \omega f(\omega) d\omega + \int_{\omega_0}^{\infty} f(\omega) d\omega \quad (23)$$

Differentiation of Eq. 23 gives

$$\frac{dI_o}{d\omega_o} = - \frac{I_{\max}}{\omega_o^2} \int_0^{\omega_o} \omega f(\omega) d\omega \quad (24)$$

and differentiation of Eq. 18 gives

$$\frac{d\omega_o}{dV_o} = - \frac{F}{KV_o^2} = - \frac{K}{F} \omega_o^2 \quad (25)$$

where

$$K = \frac{\pi[R_2^2 - R_1^2]}{2b} \quad (26)$$

and depends only on the geometry of the system. Combining Eqs. 24 and 25 gives

$$\frac{dI_o}{d\omega_o} \cdot \frac{d\omega_o}{dV_o} = \frac{dI_o}{dV_o} = I_{\max} \frac{K}{F} \int_0^{\omega_o} \omega f(\omega) d\omega \quad (27)$$

Equation 23 rearranged gives

$$\int_0^{\infty} f(\omega) d\omega = \frac{I_o}{I_{\max}} - \frac{I}{\omega_o} \int_0^{\omega_o} \omega F(\omega) d\omega \quad (28)$$

or substituting Eq. 27,

$$\int_0^{\infty} f(\omega) d\omega = \frac{I_o}{I_{\max}} - \frac{F}{\omega_o KI_{\max}} \frac{dI_o}{dV_o} \quad (29)$$

but from Eq. 18

$$\frac{F}{K\omega_o} = V_o \quad (30)$$

therefore

$$\int_{\omega_0}^{\infty} f(\omega) d\omega = \frac{I_0 - V_0 \frac{dI_0}{dV_0}}{I_{\max}} \quad (31)$$

In Eq. 29 the left side is the fraction of ions with $\omega > \omega_0$. Referring to Fig. 10 the right-hand side of the equation is the intercept on the current axis of the tangent to the voltage-current curve divided by the maximum current. Thus the current-voltage curves can be used to construct mobility distribution curves.

To relate mobility to particle size for small particles, Stokes' law is applied with a correction for slip. The relation is

$$\omega = \frac{e}{6\pi\mu} \frac{k}{r} \quad (32)$$

where μ is the viscosity of air, r is the particle radius, and e is the charge on the particle. From a review of the best data available, Davies¹³ found that the slip correction, k , for particles comparable in size to the mean free path of air molecules at room temperature was given by the expression

$$k = 1 + \frac{\lambda}{r} \left[A + B \exp \left(- \frac{Cr}{\lambda} \right) \right] \quad (33)$$

where λ is the mean free path of air and $A = 0.882$, $B = 0.281$, and $C = 1.57$.

For calculation purposes Eq. 32 is substituted into Eq. 31 to give

$$\int_{r_0}^{\infty} g(r) dr = \frac{I_0 - V_0 \frac{dI_0}{dV_0}}{I_{\max}} \quad (34)$$

where the left side is now the fraction of the total number of ions of radius $r < r_0$. Thus the size distribution of the aerosol particles can be established from the current-voltage curve by simply reading tangent intercept points for the current-voltage curve and dividing by I_{\max} to give the fraction of the size distribution with $r < r_0$.

Figure 11 shows a typical experimental current-voltage curve obtained with the ion chamber. The data plotted in this figure are for an aerosol of NaCl crystals obtained by atomizing a 0.1 per cent NaCl solution. The atomized solution droplets were first passed through a bubble chamber to remove the larger droplets and then they were evaporated to NaCl crystals by passing through a flask containing LiCl as drying agent. Next the aerosol was passed through a small version of the ion counter which served to remove the smaller ions. The results was a rather narrow distribution of approximately gaussian shape, centered close to 0.06 micron cube edge dimension. This aerosol was sampled by using a thermal precipitator and photographed with an electron microscope. A size distribution was made from the electron microscope slide.

A comparison of the size distribution obtained with the ion counter and the size distribution obtained from the electron microscope slide is shown in Fig. 5. The agreement shown here is typical for distributions sharpened such that the size range lies in the region from 0.01- to 0.1-micron "radius." For wider range distributions the agreement is not as good, since a system optimized to work best in 0.01- to 0.1-micron range is too sensitive to discriminate effectively between sizes below 0.01 micron and at the same time is too insensitive to detect effectively sizes above 0.1 micron. The system could in principle be optimized for other size ranges; however, for larger

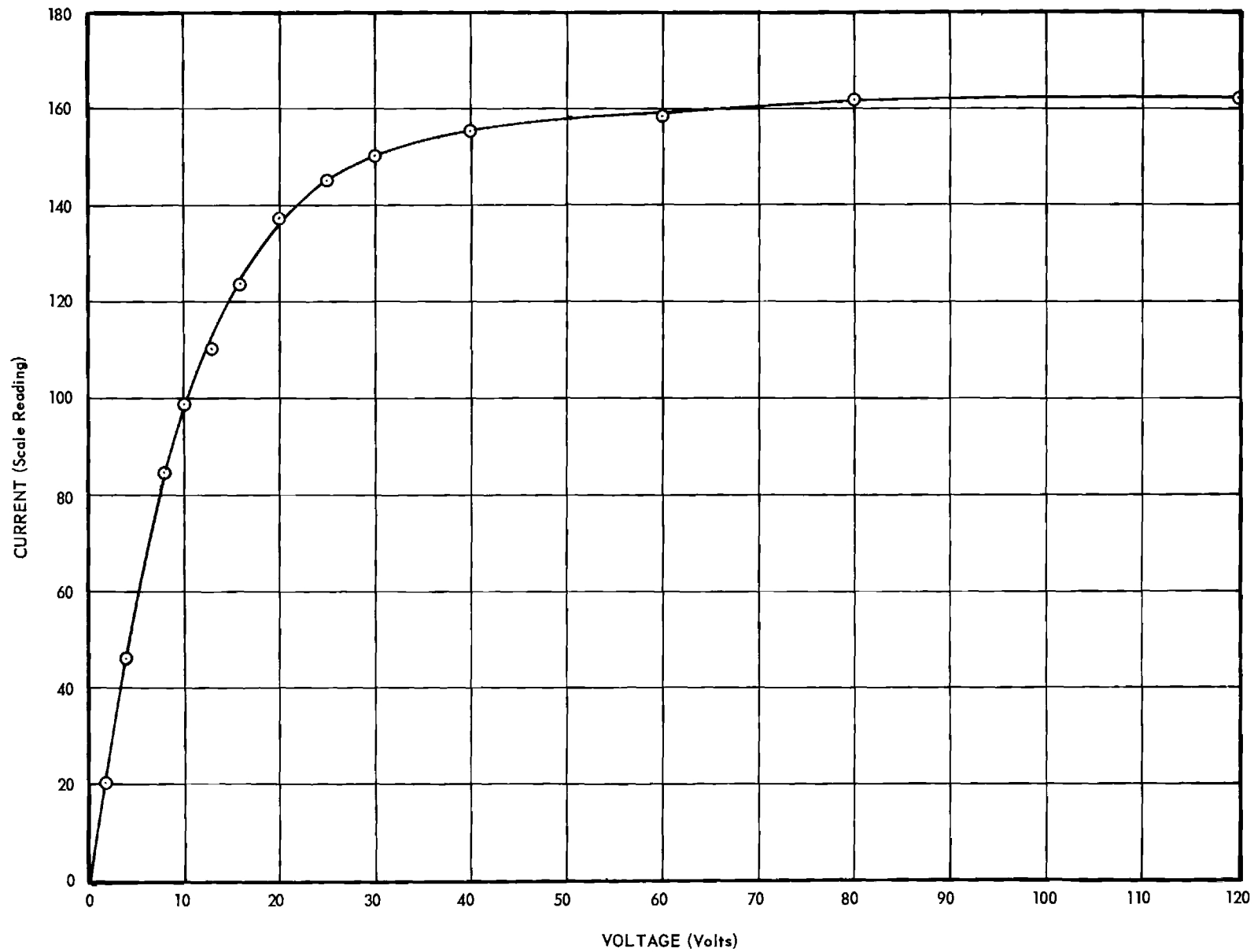


Figure 11. Experimental Current Vs. Voltage Curve for NaCl.

particles the assumption of singly charged particles upon which the entire analysis depends becomes increasingly less valid.

For aerosol processes such as those encountered in this study where the particles increase in size is due to an uptake of solvent, the absolute size change of small particles would be predicted to be less than that of larger particles. Under these conditions, the particles at any fractional point in the distribution, for example, the 50 per cent point, will remain at the same fractional point even though all particles grow.

The growth of a particular size of particle in an aerosol distribution may thus be obtained from a sequence of size distribution curves such as Figure 5 when each of the curves is for the same aerosol subjected to different conditions. For instance, a figure to be introduced later (Figure 14 in the Results section) shows an aerosol of NH_4I exposed to different vapor pressures of $\text{C}_2\text{H}_5\text{OH}$. At 23.2 per cent relative humidity the 50 per cent point size is 0.0491 micron. At 42.6 per cent relative humidity of $\text{C}_2\text{H}_5\text{OH}$ the 50 per cent point size is 0.0519 micron. Thus it may be said that a particle which had a size of 0.0491 micron at 23.2 per cent relative humidity grew to a size of 0.0519 micron when the humidity was increased to 42.6 per cent. Such an interpretation was made for all the systems at the various relative humidities as given in following tables and figures.

V. THEORETICAL PREDICTIONS OF DROPLET GROWTH

All solids in contact with a gaseous atmosphere will attract a part of the gases or vapors to their surfaces because of unsatisfied molecular forces in their surface layers. This phenomenon is called physical adsorption. The most readily condensable gases or vapors are absorbed, or held, in the greatest quantities. Temperature, partial pressure of the condensable vapors, and the nature of the solid determine the actual quantity of vapor so held.

If a particle is soluble in the vapor condensed on it, adsorption of vapor will cause the particle to gain an envelope of liquid which may become sufficient to dissolve the particle at some partial pressure of the vapor less than saturation. Prior to complete dissolution, the undissolved particle with its film of liquid will appear to the surroundings to be a droplet the concentration of which is that of a solution saturated with respect to particles of the particular size. The particle, by the same token, may be considered to be in a solution such that it behaves as it would in a solution of infinite extent having the same concentration.

The concentration of a solution in equilibrium with small crystalline particles is dependent on particle size and particle surface energy, as well as on temperature and the other usual considerations. The smaller the particle, the greater is the concentration of the saturated solution with which the particle will be in equilibrium. The relation between particle size, surface energy, and equilibrium solution concentration is given in the case of an isotropic, spherical particle by the following relationship

$$RT \ln a/a_0 = \frac{2\gamma\bar{V}}{r} \quad (35)$$

where a and a_0 are the activities of the solute in solutions of equilibrium, respectively, with a particle of radius r and a particle so large as to have essentially zero specific surface area, γ is the specific surface energy of the material and \bar{V} is the molar volume. Since the activity of the solute in solution is a measure of the solubility of the solute, this relation predicts that the smaller size of the solute particle the greater the solution concentration with which it will be in equilibrium.

As the partial pressure of the condensable vapor is increased, the envelope of liquid surrounding the particle will increase from the surrounding vapor. The extra solvent dilutes the liquid of the film so that it is no longer saturated with respect to the solid inside. As a result, more material is dissolved from the surface of the particle, thereby reducing its size. However, as the size decreases, the concentration of the solution with which the particle can be in equilibrium increases as is shown in the preceding relationship. Increased solution concentration reduces vapor pressure and causes more vapor to be condensed from the atmosphere vapor condensing again causes the droplet to grow in size.

Opposing this accretion of vapor from the surroundings is the increased vapor pressure of the volatile component in the film surrounding the particle. The relationship between the surface curvature of a droplet and its vapor pressure is expressed by the well-known Kelvin equation

$$RT \ln \frac{P_r}{P_0} = \frac{2\sigma\bar{V}}{r} \quad (36)$$

where R is the gas constant 8.32×10^7 dyne-cm/gm-mole $^{\circ}\text{K}$, T is the absolute temperature, P_r is the vapor pressure of a droplet with a radius of curvature

r , P_0 is the vapor pressure of the liquid with a surface the curvature of which is essentially zero, σ is the surface tension of the liquid, and \bar{V} is the molar volume of the liquid. The applicability of this equation to solution droplets of a volatile solvent and a nonvolatile solute, both ionic and nonionic, has been well established^{3,6} down to radii of 10^{-6} centimeters. Of course, for solutions where one of the components is sensibly nonvolatile, \bar{V} in equation (36) becomes the partial molar volume of the volatile component in the liquid state, and P_0 and σ are the vapor pressure and surface tension of the mixture, respectively.

Therefore, if the radius of curvature of the film is such that the increased vapor pressure due to curvature will exceed the vapor pressure reduction due to the presence of solute in the film, vapor will continue to condense until sufficient liquid is present completely to dissolve the particle. Once dissolution has occurred the resulting droplet will grow as the partial pressure of the volatile component in the surrounding vapor is increased in accordance with the relationship expressed by the Kelvin equation.

To calculate droplet growth with the Kelvin equation, the only data required in addition to the vapor pressure and surface tension of the mixture as a function of concentration are the solubility of the compound in the solvent and the density of the mixture as a function of concentration. The method of calculation can be outlined as follows:

(1) The mass of solute accompanying a particle of a given size is calculated from geometrical considerations using the density of the compound.

(2) The droplet sizes that would result from dissolving this quantity of solute in various quantities of the volatile solvent are calculated from

geometrical considerations using the solution densities of the corresponding concentrations.

(3) From the Kelvin equation the vapor pressure increase, P_r/P_o , due to surface curvature for each droplet size is calculated. Using these data and the normal solution vapor pressure at the corresponding concentrations, the total droplet vapor pressures are determined.

(4) Since a necessary criterion for equilibrium is that the vapor pressure of a solution droplet be equal to that of the pure vapor of the volatile component in the surrounding atmosphere, the partial pressure of the volatile component at which a droplet of a certain size can exist is determined.

The partial vapor pressure in the surrounding atmosphere necessary to cause a particle to dissolve is usually expressed as a "relative humidity" by obtaining the per cent of saturation pressure that is required. The resulting droplet size that will exist at any relative humidity can, of course, vary with the initial size of the solute particle from which it is formed. However, for a given initial particle size only one droplet size can exist at a particular relative humidity. Therefore, from calculations, droplet growth information, i.e., droplet size versus relative humidity, can be obtained for a particle of a given initial size. A theoretical growth curve for the system camphor and ethanol is given in Figure 12; Table I presents calculated data for other systems. A psychometric chart for ethanol in air is given as Figure 17 in the Appendix.¹⁴

The region representing the accretion of condensed vapor by the particulate and the point at which transition from a particulate surrounded by a film of liquid to a solution droplet occurred could not be predicted with the data

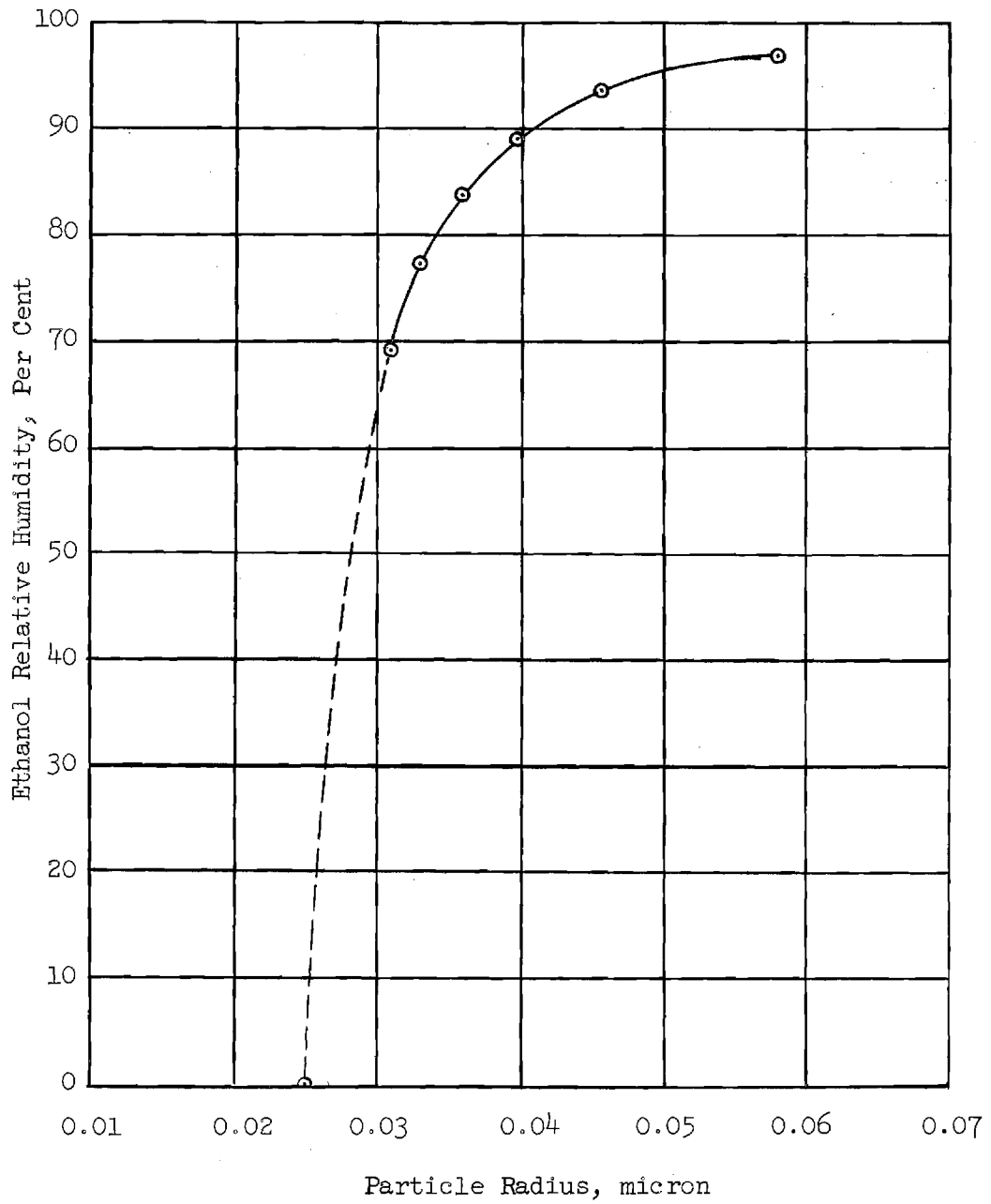


Figure 12. Theoretical Growth of a 0.025 Micron Radius Camphor Particle with Ethanol Humidity

TABLE I
CALCULATED GROWTH OF AEROSOL PARTICLES
WITH INDICATED VAPOR HUMIDITY

<u>Relative Humidity</u> (Per Cent)	<u>Particle Radius</u> (Microns)
<u>Stearic Acid and Ethanol</u>	
0	0.0250
101.09	0.0886
101.14	0.0094
101.18	0.1015
100.69	0.1116
100.64	0.1285
100.56	0.1610
0	0.0500
100.087	0.1774
100.140	0.1884
100.184	0.2030
100.217	0.2234
100.239	0.2581
100.234	0.3230
0	0.1000
99.80	0.3544
99.86	0.3768
99.93	0.4059
99.99	0.4468
100.03	0.5116
100.08	0.6445
0	0.2500
99.62	0.8862
99.69	0.9420
99.77	1.0164
99.84	1.1160
99.91	1.2785
99.98	1.6121
<u>Stearic Acid and Turpentine</u>	
0	0.0250
99.69	0.8585
99.84	0.0916
100.22	0.0987
100.45	0.1244

(continued)

TABLE I (Concluded)

CALCULATED GROWTH OF AEROSOL PARTICLES
WITH INDICATED VAPOR HUMIDITY

<u>Relative Humidity</u> (Per Cent)	<u>Particle Radius</u> (Microns)
<u>Stearic Acid and Turpentine</u>	
0	0.0500
99.03	0.1637
99.23	0.1724
99.62	0.1974
99.99	0.2487
<u>Napthalene and Gasoline</u>	
0	0.0250
85.68	0.0480
89.57	0.0530
93.61	0.0610
97.52	0.0774

available. To make estimates of this type requires data on the surface energy of the solid; this information is not available for the compounds used in these studies.

No theoretical calculations were made for the system ammonium iodide and ethanol because the validity of predicting complete growth curves for ionic salts has been demonstrated previously.^{5,6}

Contrary to the findings for systems of ionic salts, some of the organic compounds used in this work would not be predicted to grow in the presence of some vapors. This is due to the fact that the solubility of these compounds is relatively small in the volatile component and the vapor pressure lowering effect is not sufficient to overcome the vapor pressure increase produced by the sharp radius of curvature of the droplets formed. For example, a stearic acid particle with a radius of less than 0.06 micron cannot grow in the presence of ethanol vapor according to theory even when the surrounding atmosphere is saturated with ethanol vapor. This behavior was not previously observed for the systems of ionic salts because their solubility was great enough in every case to produce a sufficient vapor pressure lowering of the volatile component.

Raoult's law was employed in predicting vapor pressures as a function of concentration; this information was necessary for predicting the behavior of droplets under conditions of different relative humidity. That is, the vapor pressure of the solutions were assumed to be directly proportional to the mole fraction of the solvent. This relationship, which may be expressed as

$$\frac{P_o - P}{P_o} = \frac{n_2}{n_1 + n_2} \quad (37)$$

where P_0 is the vapor pressure of the solvent, P is the vapor pressure of the solution, and n_1 and n_2 are the number of moles of solvent and solute in the solution, respectively, has often been found surprisingly reliable for even quite concentrated solutions.

Equation 37 probably predicts the vapor pressure as a function of concentration quite well for systems where a pure one-component solvent such as ethanol was used. However, it would give only a rough approximation at best with such multi-component solvents as gasoline or turpentine. Since the direct measurement of the vapor pressures of solutions prepared with these solvents was beyond the scope of this problem, Raoult's law was deemed the best method for obtaining estimates of vapor pressures. In the case of gasoline the product used was Amoco, and an average boiling point of 93.3°C was obtained for this gasoline through the courtesy of the American Oil Company. With the average boiling point and an empirical relationship between the vapor pressure P and the absolute temperature T of gasoline¹⁵

$$\frac{d(\log P)}{d\left(\frac{1}{T}\right)} = 1650 \quad (38)$$

the vapor pressure at 25°C was estimated. In the case of turpentine which is approximately 80 per cent α -pinene,¹⁶ the vapor pressure of α -pinene at 25°C was taken as representing the vapor pressure of turpentine.

VI. RESULTS

A. Gasoline Exhaust

Particulate size distributions obtained for the exhaust of a small 4-cycle engine as described in Section III A3a are given in Table II and a typical electron micrograph of the aerosol is shown in Figure 13. The results indicate "smog" formation from the products of the engine exhaust.

B. Aerosols Produced by Ethanol Solution Atomization

Stearic acid, camphor, and ammonium iodide aerosols were produced by atomizing dilute ethanol solutions of these compounds. The aerosol streams were then heated to approximately 50°C to lower the relative humidity and to assure that solid particles were formed, while the alcohol was removed from the systems by a series of cold traps. The aerosols then passed through a temperature-controlled bath, where the desired amounts of turpentine, ethanol, or dioctylphthalate vapors were added. The aerosol and vapor system then passed to a second bath to lower the relative humidity, and through an aging chamber, where the temperature was reduced. (This assured that the aerosol always passed from a condition of lower to higher relative humidity.) Ions were introduced into the system in the latter chamber also to produce an electrical charge on the aerosol. The aerosol, finally, was led into the ion counter.

The vapor concentration or the relative humidity for the above systems, other than those of stearic acid and turpentine and ammonium iodide and dioctylphthalate, were determined by dew point measurements. The amount of turpentine was determined by condensing the vapor for a given time interval and weighing it; the aerosol size change was thus determined in terms of a weight per cent of turpentine. Results of the dioctylphthalate and ammonium

TABLE II

TYPICAL SIZE DISTRIBUTIONS OBTAINED FROM GASOLINE ENGINE EXHAUST

Per Cent Less Than Indicated Size	Particle Radius			
	Regular Gasoline			Unleaded Gasoline
	Distribution 1 ^a (Microns)	Distribution 2 ^b (Micron)	Distribution 3 ^c (Micron)	Distribution 4 ^a (Micron)
20	0.043	0.054	0.056	0.038
30	0.050	0.062	0.067	0.041
40	0.056	0.069	0.081	0.044
50	0.060	0.079	0.097	0.047
60	0.064	0.091	0.114	0.050
70	0.068	0.105	0.140	0.053
80	0.072	0.123	0.172	0.056
90	0.080	--	--	0.059

^a Aerosol was taken direct from engine exhaust without aging.

^b Aerosol was passed through aging chamber without irradiation. Average time in chamber was one hour.

^c Aerosol was passed through aging chamber with irradiation. Average time in chamber was one hour.

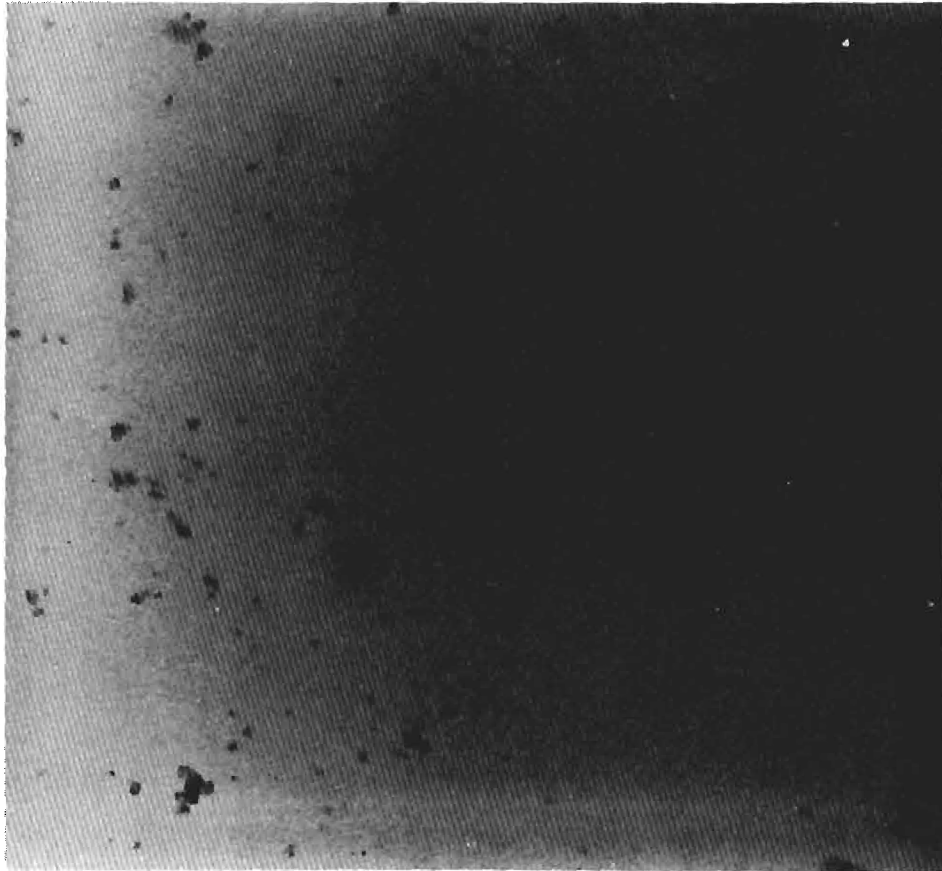


Figure 13. Electron Micrograph of Particulate Matter from Gasoline (Unleaded) Engine Exhaust. (1 Millimeter = 1 Micron)

iodide system were obtained as a function of the temperature at which the dioctylphthalate was maintained.

Current versus voltage measurements for these systems are given in Tables XIII through XVII in the Appendix and particulate size distributions for the various systems are given in Tables III through VII. Figure 14 shows a series of size distributions for an ammonium iodide aerosol exposed to several concentrations of ethanol.

C. Paraffin Aerosol

Paraffin aerosols were generated by atomizing dilute solutions of paraffin and hexane. The hexane vapor produced during aerosol generation was partially removed from the aerosol by condensation in a cold trap. The desired amount of hexane vapor was then added to the system by passing the aerosol over liquid hexane at a controlled temperature. This system was employed because it afforded better control over vapor concentration. Since paraffin melts at a rather low temperature the stream was only heated slightly to ensure an increasing relative humidity situation. The aerosol was next passed through an aging chamber, where an electrical charge was induced, and then into the ion counter. The current versus voltage measurements are given in Table XVIII in the Appendix. The size distributions for particular hexane concentrations are given in terms of the temperature of the hexane bath in Table VIII.

D. Naphthalene Aerosol

Naphthalene was generated and treated in the same manner as paraffin until it reached the aging chamber, except that gasoline vapor was employed instead of hexane. The naphthalene aerosol was sufficiently charged by the generation process and additional charging was not required. The current

TABLE III

SIZE DISTRIBUTIONS OBTAINED FOR SYSTEMS OF STEARIC ACID AND ETHANOL

Particle Radius (micron)	Per Cent of Particulates Less than Indicated Size at Ethanol Relative Humidities of									
	48%	57%	64%	69%	71%	75%	76%	77%	78%	79%
0.0154	3.5	3.6	4.3	5.1	3.6	3.7	3.2	2.7	5.4	5.4
0.0226	12.0	9.4	10.5	12.2	10.3	9.6	10.2	7.7	14.6	12.3
0.0282	21.7	16.2	17.4	22.4	19.9	20.2	19.6	13.3	22.5	23.1
0.0327	29.7	24.1	27.7	33.5	27.5	27.4	26.1	21.4	29.1	35.2
0.0369	35.9	31.1	35.6	40.1	37.5	36.6	33.8	31.4	38.4	47.6
0.0407	43.1	39.3	40.3	47.0	44.9	44.8	39.0	39.2	43.9	56.2
0.0444	52.4	46.6	46.3	52.3	52.5	50.7	44.8	45.4	49.4	60.5
0.0479	58.8	51.5	52.7	58.0	58.3	57.7	52.2	50.5	55.3	64.0
0.0512	65.6	55.9	59.4	62.8	64.4	63.1	58.1	53.4	60.3	66.9
0.0546	67.1	59.0	63.2	66.3	68.9	66.8	62.1	56.8	64.5	69.3
0.0578	68.3	61.4	66.2	69.6	72.8	69.7	65.6	64.2	66.7	71.3
0.0608	70.2	65.7	69.5	71.8	74.1	72.5	68.1	70.0	79.0	73.8
0.0666	74.3	71.2	73.1	76.4	76.2	76.4	72.3	76.5	72.7	77.0
0.0722	77.2	76.1	77.3	79.8	77.3	79.4	79.9	81.0	75.6	79.4
0.0776	79.2	81.1	80.2	82.7	78.5	81.9	88.4	85.8	77.8	81.8
0.0830	81.5	85.9	82.4	85.9	80.9	85.1	92.0	90.7	81.3	84.6
0.0883	87.2	--	84.3	87.9	83.2	86.9	95.3	94.0	84.6	86.7
0.0934	91.5	89.8	86.9	88.8	84.9	88.0	98.3	95.8	86.5	88.0

TABLE IV

SIZE DISTRIBUTIONS OBTAINED FROM SYSTEMS OF CAMPHOR AND ETHANOL

Particle Radius (micron)	Per Cent of Particulates Less than Indicated Size of Ethanol Relative Humidities of							
	<u>27%</u>	<u>35%</u>	<u>39%</u>	<u>54%</u>	<u>56%</u>	<u>68%</u>	<u>71%</u>	<u>91%</u>
0.0164	9.8	--	8.2	12.7	12.1	17.4	12.6	11.7
0.0238	25.0	23.8	23.0	26.9	35.1	32.9	27.2	25.8
0.0298	36.8	38.0	37.1	42.3	47.3	42.7	39.8	36.7
0.0347	48.7	48.4	51.5	53.8	55.4	53.1	49.2	44.7
0.0392	56.8	57.9	61.3	60.3	60.7	64.6	58.2	52.4
0.0434	63.6	67.1	66.4	64.9	66.7	70.7	69.5	58.1
0.0474	68.2	73.8	69.5	69.6	75.6	75.7	72.8	62.5
0.0510	72.9	76.6	75.3	73.5	80.4	78.4	76.9	65.3
0.0547	77.9	79.6	80.4	76.9	83.4	82.2	79.7	68.9
0.0582	84.3	81.3	84.4	80.3	85.2	84.2	81.7	72.6
0.0648	88.2	85.9	89.9	84.2	88.8	86.1	86.5	77.4
0.0712	89.8	87.1	91.4	87.2	91.9	86.9	89.4	80.7
0.0774	91.1	87.9	93.0	88.0	94.8	87.1	92.3	83.4
0.0892	94.1	--	96.5	--	96.2	90.1	--	--
0.1004	97.5	--	97.6	93.9	--	--	--	--

TABLE V

SIZE DISTRIBUTIONS OBTAINED FROM SYSTEMS OF AMMONIUM IODIDE AND ETHANOL

Particle Radius (micron)	Per Cent of Particulates Less than Indicated Size at Ethanol Relative Humidities of							
	23%	38%	41%	43%	53%	61%	67%	70%
0.0154	3.1	2.0	1.2	1.4	1.4	1.3	--	--
0.0226	8.0	6.6	8.1	5.6	4.3	3.4	1.5	--
0.0282	15.7	13.7	16.5	14.1	9.9	7.5	2.6	--
0.0327	20.7	21.5	23.6	19.4	16.7	12.2	4.6	0.9
0.0369	29.2	26.6	28.3	25.1	21.3	16.0	7.1	--
0.0407	37.1	30.9	33.5	31.7	26.5	19.6	11.0	3.1
0.0444	40.3	37.3	41.0	36.3	32.8	22.5	15.5	--
0.0479	45.2	45.9	47.5	41.3	39.2	24.5	18.8	6.5
0.0512	54.1	53.0	52.4	48.4	45.7	27.9	21.8	8.4
0.0546	61.5	60.0	56.6	56.2	53.3	32.6	26.1	10.7
0.0578	68.4	65.0	59.4	63.4	59.1	42.2	31.7	14.2
0.0608	73.5	68.5	62.3	66.8	63.9	53.0	37.8	18.9
0.0666	80.0	74.6	69.2	71.7	70.2	62.4	48.6	30.7
0.0722	81.8	79.2	75.1	77.7	74.8	68.2	55.2	40.7
0.0776	83.4	83.0	79.7	80.9	76.9	71.3	58.8	48.7
0.0830	85.5	85.8	83.3	84.3	80.0	74.2	62.9	54.5
0.0883	88.3	89.1	86.5	88.2	--	77.9	66.6	57.9
0.0934	90.8	90.4	88.1	90.2	82.7	80.7	70.0	62.6

TABLE VI

SIZE DISTRIBUTIONS OBTAINED FROM SYSTEMS OF STEARIC ACID AND TURPENTINE

Particle Radius (micron)	Per Cent of Particulates Less than Indicated Size at Turpentine Weight Fractions of											
	0.0	0.287	0.368	0.381	0.437	0.481	0.521	0.555	0.561	0.580	0.581	0.600
0.0226	3.4	2.4	2.0	2.8	1.8	2.3	2.1	4.6	1.6	2.6	2.3	2.4
0.0282	8.1	4.9	3.9	6.0	4.0	6.3	4.6	10.8	5.1	7.3	4.5	5.9
0.0327	14.8	10.0	7.3	9.6	8.5	9.9	9.1	19.5	10.8	13.3	7.7	9.9
0.0369	22.2	17.2	11.3	14.2	13.3	14.9	15.1	26.6	18.9	20.0	10.7	13.5
0.0407	27.2	24.1	15.1	18.6	18.1	21.7	21.3	33.7	26.3	27.1	14.3	16.5
0.0444	32.0	28.7	19.5	24.8	22.1	28.8	25.9	39.1	33.0	35.0	19.0	19.6
0.0479	38.4	32.3	25.6	31.9	29.2	32.4	29.7	49.1	36.9	39.7	24.9	23.7
0.0512	43.8	37.6	34.7	37.7	34.0	35.9	32.0	57.8	42.0	43.1	29.8	29.4
0.0546	49.8	43.9	39.6	43.6	38.9	41.7	35.7	63.7	46.4	47.0	34.3	35.7
0.0608	57.0	56.8	46.6	54.4	50.1	54.7	45.3	72.7	53.0	54.3	46.3	44.4
0.0666	63.6	63.9	54.0	65.6	58.2	62.4	54.7	79.0	64.4	66.9	52.9	49.1
0.0722	69.0	69.0	63.9	71.0	67.6	67.5	61.2	82.7	70.3	76.4	58.5	51.9
0.0776	73.0	73.0	70.2	75.5	73.3	71.5	65.1	86.3	75.5	82.0	63.1	56.3
0.0830	77.2	77.3	74.7	81.0	76.3	74.8	69.1	90.6	79.8	88.6	67.1	59.7
0.0883	80.8	81.0	80.4	85.7	80.0	78.1	73.2	94.0	83.9	93.8	69.9	63.6
0.0934	83.7	84.6	87.4	88.8	84.8	81.2	76.3	96.3	87.8	96.1	74.4	68.7
0.1317	100.0	100.0	100.0	100.0	100.0	100.0	100.0	100.0	100.0	100.0	100.0	100.0

TABLE VII

SIZE DISTRIBUTIONS OBTAINED FROM SYSTEMS OF AMMONIUM IODIDE AND DIOCTYLPHTHALATE

Particle Radius (micron)	Per Cent of Particulates Less than Indicated Size as Generated	Per Cent of Particulates Less than Indicated Size at Dioctylphthalate Vapor Concentrations Resulting from Bath Temperatures of			
		28.8°C	35.0°C	48.1°C	73.2°C
0.0226	--	--	2.2	1.7	1.8
0.0327	5.9	5.0	7.9	6.1	5.7
0.0407	19.9	12.3	18.6	12.8	13.3
0.0444	26.0	16.7	21.8	19.3	16.9
0.0479	30.9	23.2	25.3	26.6	22.5
0.0512	34.8	31.1	30.1	33.9	28.3
0.0546	38.6	38.6	35.8	40.8	35.4
0.0578	42.5	44.5	--	45.3	38.8
0.0608	47.8	50.6	43.1	48.5	42.2
0.0637	--	57.9	--	52.3	46.5
0.0666	57.4	62.5	48.2	57.0	50.3
0.0694	--	--	--	61.1	54.5
0.0722	63.4	68.3	54.5	65.4	58.8
0.0776	65.9	74.8	63.5	70.3	65.2
0.0830	68.9	80.1	68.4	74.3	70.2
0.0883	72.5	84.3	73.4	79.6	74.4
0.0934	77.9	88.8	78.7	82.7	78.7

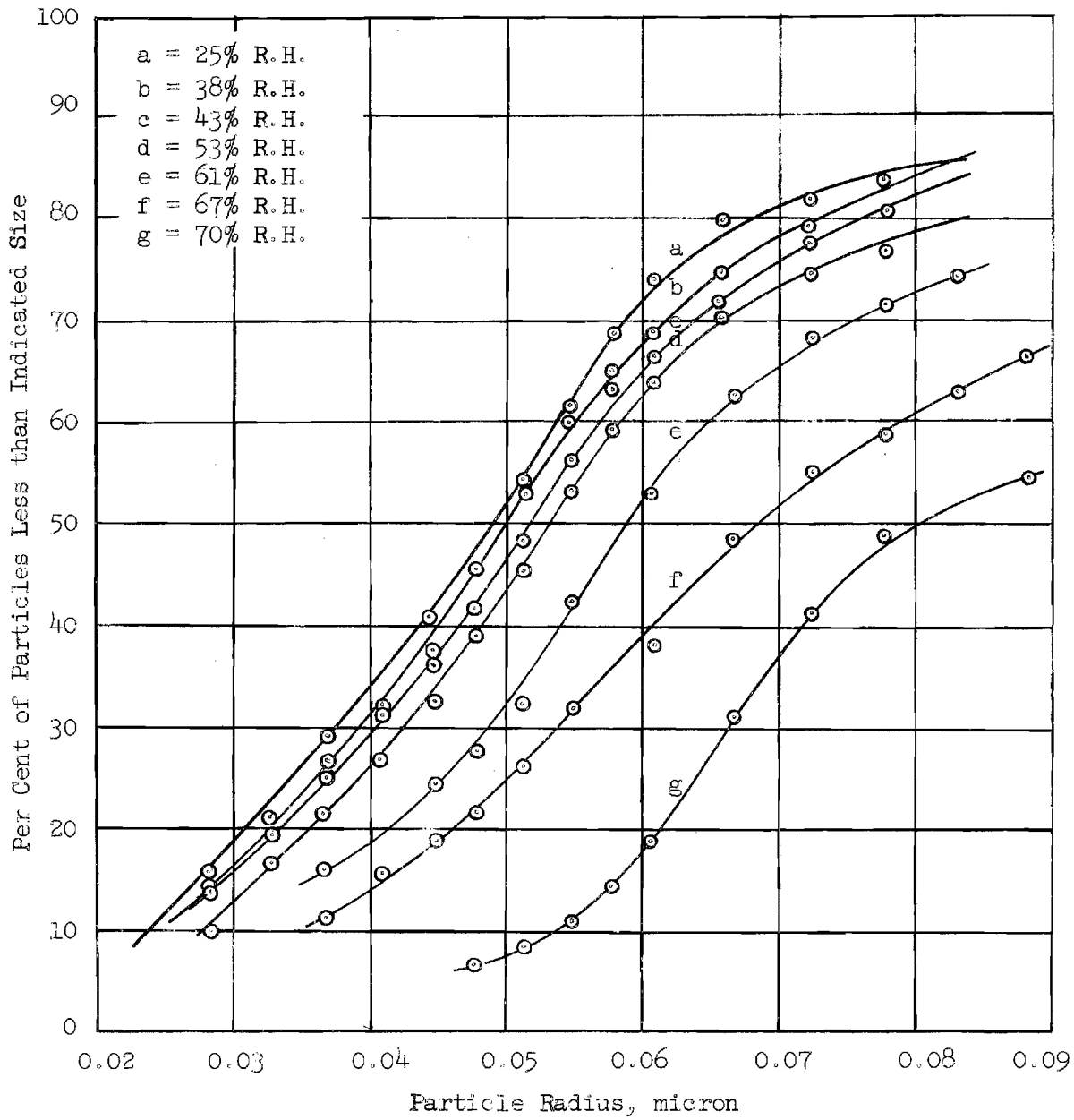


Figure 14. Size Distributions Obtained from Ammonium Iodide and Ethanol Systems

TABLE VIII

SIZE DISTRIBUTIONS OBTAINED FROM SYSTEMS OF PARAFFIN AND HEXANE

<u>Particle Radius</u> (microns)	<u>Per Cent of Particulates Less than Indicated Size at Hexane Bath Temperatures of</u>		
	<u>24.6°C</u>	<u>47.8°C</u>	<u>76.3°C</u>
0.0226	3.7	6.7	10.8
0.0282	8.4	12.8	22.2
0.0327	15.3	21.0	31.8
0.0369	26.6	28.2	40.8
0.0407	38.5	36.8	47.9
0.0444	48.0	45.5	54.4
0.0479	54.7	56.0	60.2
0.0512	63.5	64.1	64.8
0.0546	70.8	70.0	68.4
0.0578	76.8	76.2	72.8
0.0608	81.9	81.8	79.3
0.0637	84.9	85.4	83.0
0.0666	87.1	88.1	87.3
0.0694	89.9	90.8	91.0
0.0722	91.7	--	95.1
0.0760	95.4	--	--

voltage data are given in Table XIX in the Appendix. Size distributions as made for various concentrations of gasoline are given in terms of the temperature of the controlled gasoline bath in Table IX.

E. Carbon and Graphite Aerosols

A graphite aerosol was generated by the exploding wire technique and drawn into a mixing chamber. There the aerosol was mixed with a fan for several minutes and allowed to equilibrate and then to settle for several hours. The aerosol was forced at the end of this time from the mixing chamber through another system of chambers consisting of two identical mixing chambers arranged in parallel. One chamber contained a small quantity of liquid benzene and the other was completely empty except for air. The voltage applied to the electrode of the ion counter was set to collect approximately half of the total number of ions, and the aerosol stream was passed through the empty chamber a few minutes and then through the chamber containing benzene. The entire procedure was repeated a number of times. Never was a change in ion current detected, therefore there must have been no change in aerosol size.

Carbon was treated in an identical manner except for the method of generation. The carbon aerosol was produced by burning a mixture of benzene and alcohol as described previously. Again there was no change in ion current after being exposed to benzene and, therefore there must have been no change in aerosol size.

F. Poly(Methyl Methacrylate) Aerosol

Poly(Methyl Methacrylate) aerosol was generated as previously described with the polymer aerosol generator. An electrical charge was induced on the aerosol with the ion generating device. The aerosol was then passed over

TABLE IX

SIZE DISTRIBUTIONS OBTAINED FROM SYSTEMS OF NAPHTHALENE AND GASOLINE

Particle Radius (Microns)	Per Cent of Particulates Less than Indicated Size at Gasoline Bath Temperatures of					
	<u>24.8°C</u>	<u>25.1°C</u>	<u>31.5°C</u>	<u>37.2°C</u>	<u>54.6°C</u>	<u>60.0°C</u>
0.0154	11.7	8.7	5.2	12.8	6.6	2.8
0.0226	30.0	19.3	25.3	32.6	11.2	6.5
0.0282	45.5	33.3	42.1	46.8	30.1	17.2
0.0327	58.7	43.3	55.0	61.2	46.8	27.1
0.0369	72.6	62.2	67.8	72.6	57.8	46.3
0.0407	80.5	75.5	75.5	81.1	71.7	55.7
0.0444	86.4	82.9	79.0	86.5	81.6	62.7
0.0479	89.1	88.8	81.4	91.6	89.4	73.4
0.0512	91.7	92.2	82.9	93.0	95.1	80.9
0.0546	92.9	94.2	86.2	94.6	98.2	85.5
0.0578	95.7	96.2	89.6	97.3	--	88.1
0.0608	99.5	--	91.4	--	--	90.7

liquid methyl ethyl ketone in a temperature-controlled chamber, through an aging chamber, and into the ion counter. Current versus voltage data were taken without exposing the aerosol to the ketone and then following exposure to desired ketone concentrations. The results are given in Table XX in the Appendix. The size distributions at various humidities are given in Table X. Figure 15 shows the change in aerosol size as a function of the methyl ethyl ketone relative humidity. The poly(methyl methacrylate) aerosol was also investigated using acetone vapor. The procedure was the same as with the methyl ethyl ketone. Figure 16 shows a comparison of the aerosol radius with no acetone vapor and with a high relative humidity of acetone.

G. Synthetic "Smog"

Synthetic "smog" was produced by irradiating a mixture of NO_2 , SO_2 , and 1-pentane in air with ultraviolet light. No increase in smog particulate size was detected upon exposing the smog to a high concentration of benzene vapor.

H. Physical Properties

Solubility and surface tension data for the systems investigated are given in Tables XI and XII.

TABLE X

SIZE DISTRIBUTIONS OBTAINED FROM SYSTEMS OF POLY(METHYL METHACRYLATE)
AND METHYL ETHYL KETONE

Particle Radius (micron)	Per Cent of Particulates Less than Indicated Size at Ketone Relative Humidities of									
	Test 1		Test 2		Test 3		Test 4		Test 5	
	0%	33%	0%	34%	0%	43%	0%	47%	0%	48%
0.0154	36.9	19.9	4.2	9.3	16.6	4.8	6.7	8.1	43.5	14.3
0.0226	56.9	42.9	15.9	20.5	31.3	19.3	27.8	18.1	64.8	28.4
0.0282	69.1	57.8	25.7	28.7	35.9	30.0	44.1	24.2	72.2	38.9
0.0327	78.4	68.7	38.6	35.3	47.1	45.6	54.7	29.9	78.9	45.6
0.0369	84.2	76.9	55.8	43.2	65.7	53.5	62.5	34.5	83.4	51.1
0.0407	89.8	81.5	75.5	51.7	79.8	59.8	74.9	38.0	85.7	57.4
0.0444	94.2	85.9	84.2	57.7	90.3	--	89.7	40.8	89.3	63.4
0.0479	97.8	89.5	94.2	64.2	96.8	69.6	--	43.5	93.3	68.7
0.0512	--	94.0	--	70.7	--	--	--	--	97.6	72.9
0.0546	--	96.9	--	76.3	--	76.5	--	48.0	--	75.4
0.0578	--	--	--	80.0	--	--	--	--	--	--
0.0608	--	--	--	83.7	--	81.7	--	55.4	--	--
0.0666	--	--	--	89.3	--	85.7	--	69.9	--	--
0.0722	--	--	--	94.7	--	89.6	--	79.3	--	--
0.0776	--	--	--	--	--	--	--	87.5	--	--

(Continued)

TABLE X (Continued)

SIZE DISTRIBUTIONS OBTAINED FROM SYSTEMS OF POLY(METHYL METHACRYLATE)
AND METHYL ETHYL KETONE

Particle Radius (micron)	Per Cent of Particulates Less than Indicated Size at Ketone Relative Humidities of									
	Test 6		Test 7		Test 8		Test 9		Test 10	
	0%	54%	0%	55%	0%	60%	0%	67%	0%	75%
0.0154	10.8	2.2	17.6	--	35.0	7.0	35.5	11.1	39.1	3.8
0.0226	36.9	7.9	41.8	4.5	55.7	21.2	59.1	26.8	59.3	21.2
0.0282	64.0	15.4	61.3	15.2	69.8	34.7	76.4	39.0	68.8	34.9
0.0327	76.1	22.3	76.9	26.7	78.0	45.9	89.0	48.7	76.7	44.9
0.0369	79.6	27.4	84.2	46.2	83.6	57.8	--	59.5	84.0	52.7
0.0407	82.9	30.9	91.6	58.6	88.7	68.6	--	66.6	91.9	59.5
0.0444	86.8	--	94.9	65.2	92.3	75.4	--	72.6	--	65.3
0.0479	90.1	36.0	--	70.0	95.9	80.7	--	77.4	--	71.3
0.0512	--	--	--	74.5	--	--	--	--	--	--
0.0546	94.1	42.6	--	80.2	--	88.0	--	81.9	--	79.2
0.0578	--	46.9	--	82.9	--	--	--	--	--	--
0.0608	--	52.3	--	85.2	--	94.3	--	86.6	--	84.1
0.0666	--	66.0	--	83.3	--	--	--	90.3	--	89.0
0.0722	--	76.3	--	93.6	--	--	--	94.4	--	91.9
0.0776	--	82.6	--	--	--	--	--	98.1	--	--

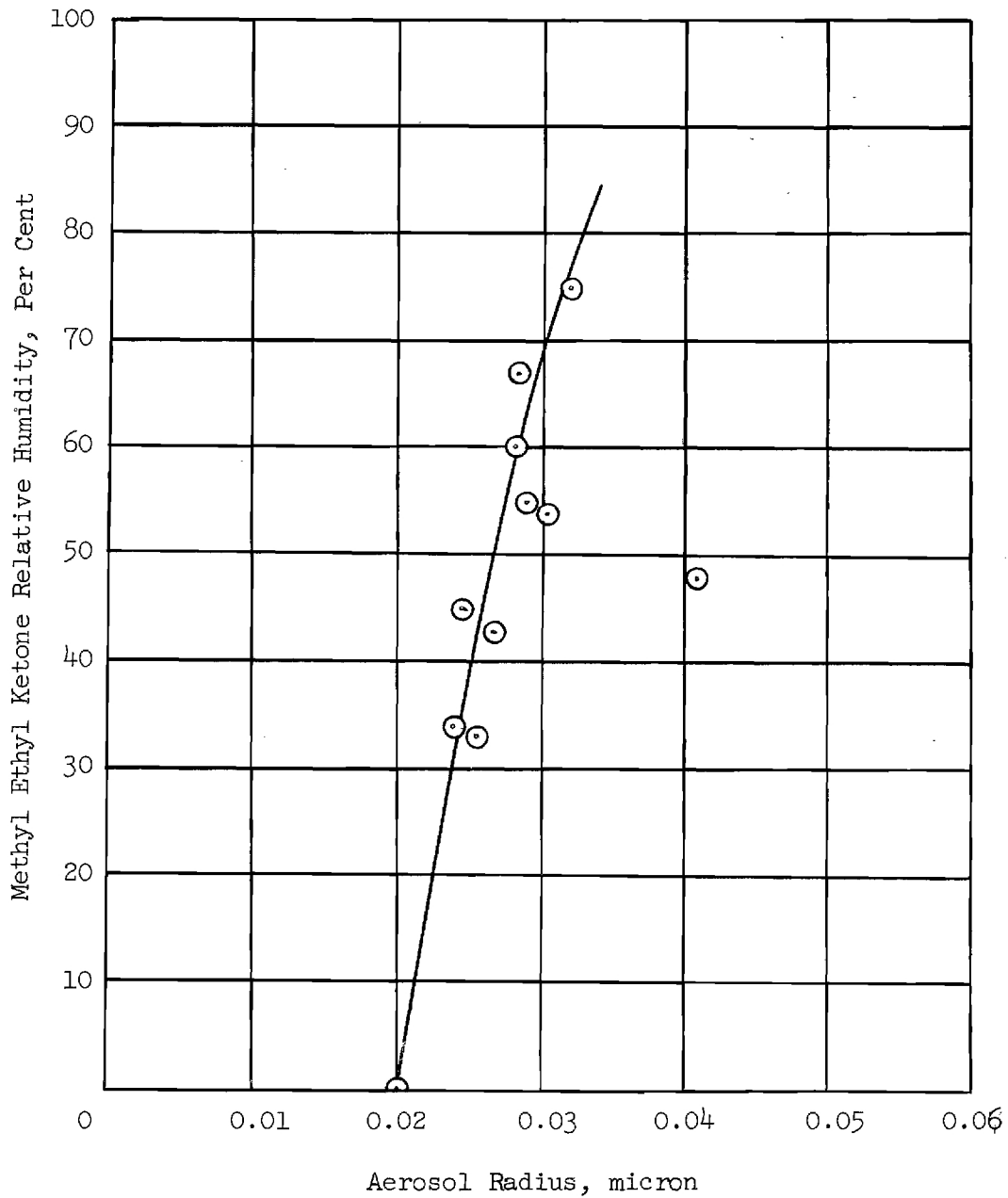


Figure 15. Experimental Growth Curve for a 0.02 Micron Radius Poly(Methyl Methacrylate) Particle with Increasing Methyl Ethyl Ketone Relative Humidity

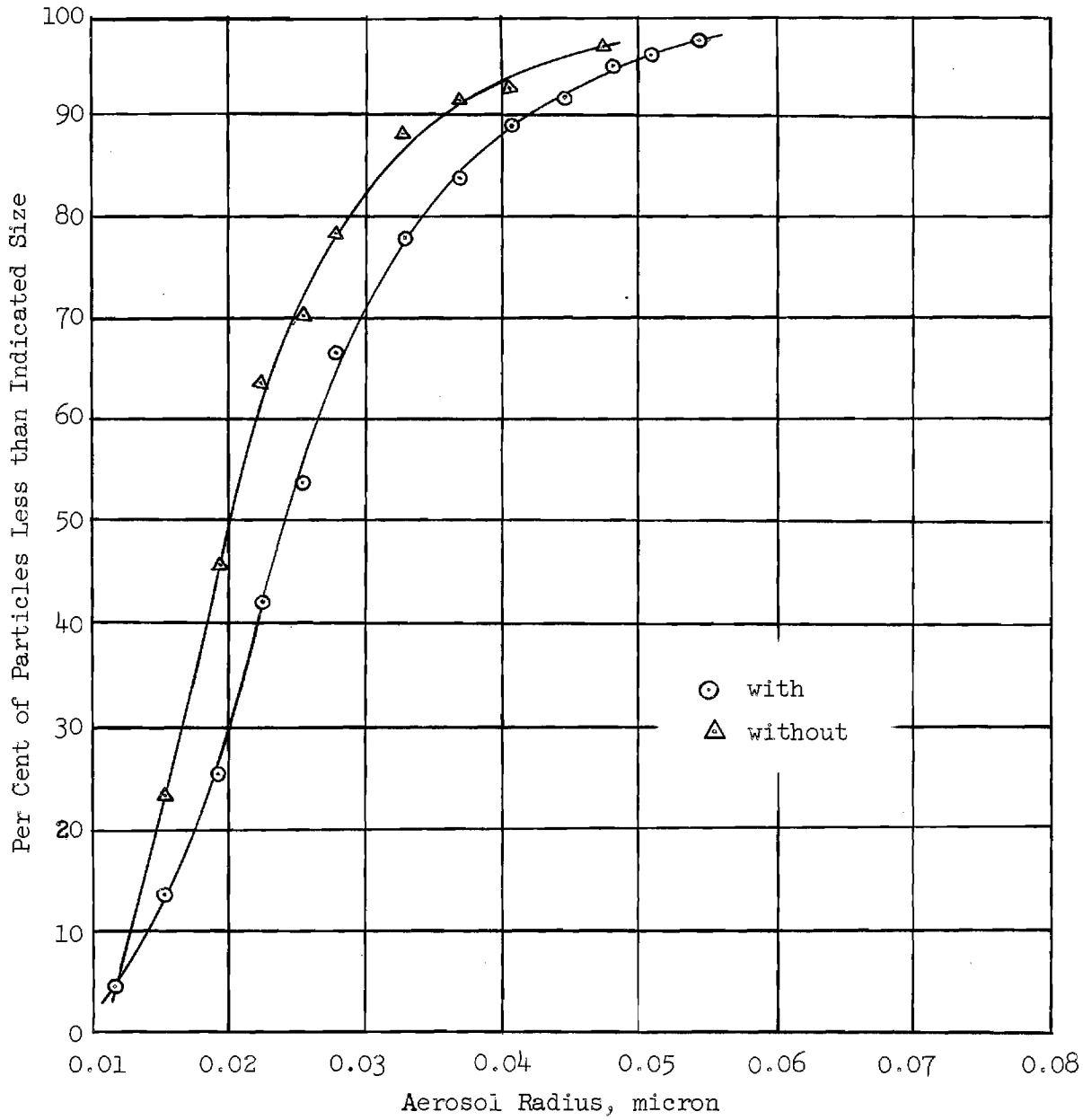


Figure 16. Comparison of Poly(Methyl Methacrylate) Aerosol Size Distributions Obtained with No Acetone Vapor and in an Atmosphere Very Nearly Saturated with Acetone

TABLE XI
SOLUBILITY DETERMINATIONS

System		Solubility at 25° C (Gm/100 gm solvent)
Solid	Solvent	
Stearic Acid	Ethanol	4.8
Camphor	Ethanol	155.0
Napthalene	Gasoline	32.0
Stearic Acid	Turpentine	4.5
Poly(Methyl Methacrylate)	Methyl Ethyl Ketone	51.0
*Ammonium Iodide	Ethanol	26.3
*Paraffin	Benzene	1.99

*Atherton Seidell, Solubilities of Inorganic and Organic Compounds,
Vol. 1, Second edition, Van Nostrand, New York, 1919.

TABLE XII
SURFACE TENSION OF SOLUTIONS

<u>Concentration</u> (Weight %)	<u>Surface Tension</u> (Dynes/Cm ²)
<u>Stearic Acid and Ethanol</u>	
0.5	22.028
1.0	22.045
1.5	22.070
2.0	22.101
2.5	22.137
3.0	22.180
<u>Stearic Acid and Turpentine</u>	
1.0	26.54
2.0	26.93
3.0	27.45
3.5	27.72
<u>Napthalene and Gasoline</u>	
5	21.525
10	21.945
15	22.66
20	23.38
<u>Camphor and Ethanol</u>	
10	22.37
20	22.96
30	23.74
40	24.66
50	25.64
60	26.68

VII. DISCUSSION OF RESULTS

The results from the studies of gasoline exhaust, presented in Table II, show that practical aerosol size analyses can be made with an ion counter. A particular result gives, for example, that a particle of 0.060-micron radius taken directly from the engine exhaust grew to 0.079 micron after being aged for a period of one hour and to 0.097 micron after being irradiated with ultraviolet light for one hour. Table II also shows that the distribution obtained for unleaded gasoline exhaust was somewhat smaller than that obtained with leaded gasoline. Reproducible aerosols could not always be obtained because several of the variables could not be sufficiently controlled. Engine speed, temperature, fuel mixture, humidity, and air intake temperature all affected the aerosol output and of these the most serious appeared to be engine speed. The engine not only influenced the particle size directly but it altered the aerosol flow rate in the system.

Aerosols of nonionic substances such as stearic acid, poly(methyl methacrylate), and camphor are normally uncharged when produced by solution atomization, hence their size distribution could not be determined with the ion counter until the aerosol charging device was constructed. The device worked quite satisfactorily for long periods. The results of this phase of the investigation indicate that particulate aerosols will show significant size increases when exposed to less than 100 per cent relative humidities of vapors of liquids in which the aerosols are sufficiently soluble. The process is concluded to be one in which the solid first dissolves in the adsorbed solvent to become a solution droplet at a relative humidity which, in principle, can be calculated from the surface energy of the solid, and the surface tension

and vapor pressure of the solution. Unfortunately, data for these calculations are not available for most organic materials in organic solvents, including many of those investigated in this study. However, theory predicts that, in general, the more soluble materials will become solution droplets at lower relative humidities. The results obtained in this investigation are in agreement with this prediction. For instance, the graphite and benzene and the carbon and benzene systems which are completely insoluble showed no measureable size increase. In the cases of the stearic acid and alcohol, stearic acid and turpentine, paraffin and benzene, and naphthalene and gasoline systems, the solubilities are relatively low and therefore the vapor pressure lowering effect of the solute is small. Hence these systems would be predicted to show little or no size increase except at extremely high relative humidities, which is in agreement with experimental results. The systems which showed considerable size change were those consisting of ammonium iodide and ethanol, poly(methyl methacrylate) and methyl ethyl ketone, and camphor and ethanol. Here the solubility of the aerosol material in the vaporous component is high and the resulting solution has a vapor pressure significantly lower than that of the pure solvent. Hence, again theory and experiment are in agreement in indicating quite significant size changes for these systems.

The "affinity" tests in which pieces of the aerosol material were exposed to a 100 per cent vapor relative humidity was a qualitative experiment to indicate the possibility of size change. It might be refined to give more quantitative data by noting the rate of vapor pickup.

An estimate of the consistency of the data and results may be obtained by examining Figure 15. The deviations from a single line indicated in this

figure are typical. The largest single contribution to deviation was a fluctuation in the aerosol flow rate. The electrical equipment associated with the ion counter was extremely stable and free of noise, hence its contribution to deviation was negligible.

Synthetic "smog" was found to be readily produced by irradiating a mixture of nitrogen dioxide, sulfur dioxide, and 1-pentane in air with ultraviolet light without the specific addition of inert nuclei. This is in general agreement with the findings of others.^{9,18} In order to achieve sufficient ion current for analysis, a minimum gas flow of 60 cc/sec was required. The average residence time in available chambers was insufficient to produce the aerosol continuously at this flow rate, therefore tests with this aerosol were obtained only periodically. This restricted the time available for making measurements. Also, the aerosols produced in this fashion contained larger size particulates than can accurately be analyzed in an ion counter and absolute size determinations could not be made. However, a change in aerosol size could easily be detected. It may be noted that exposure of this "smog" to organic vapors in the absence of irradiation produced no detectable size changes but an increase was occasioned by increases in water vapor content of the mixture being irradiated.

VIII. CONCLUSIONS

From the results of this investigation it may be concluded that:

1. Particulate aerosols that are soluble in volatile organic solvents increase in size with increase in solvent vapor concentrations. The extent of the size change may be predicted from theoretical considerations.

2. In general, the greater the solubility of the aerosol material the lower will be the relative humidity at which significant growth will occur.

3. For materials with a relatively low solubility (less than approximately 5 per cent by weight) relative humidities in excess of 100 per cent are required for growth if the nuclei size is of the order of 0.01 micron diameter.

4. An ion counter affords an excellent means for analyzing aerosol particulate radii in the range from 0.01 to 0.1 micron.

X. APPENDIX

A. References

B. Psychometric Chart

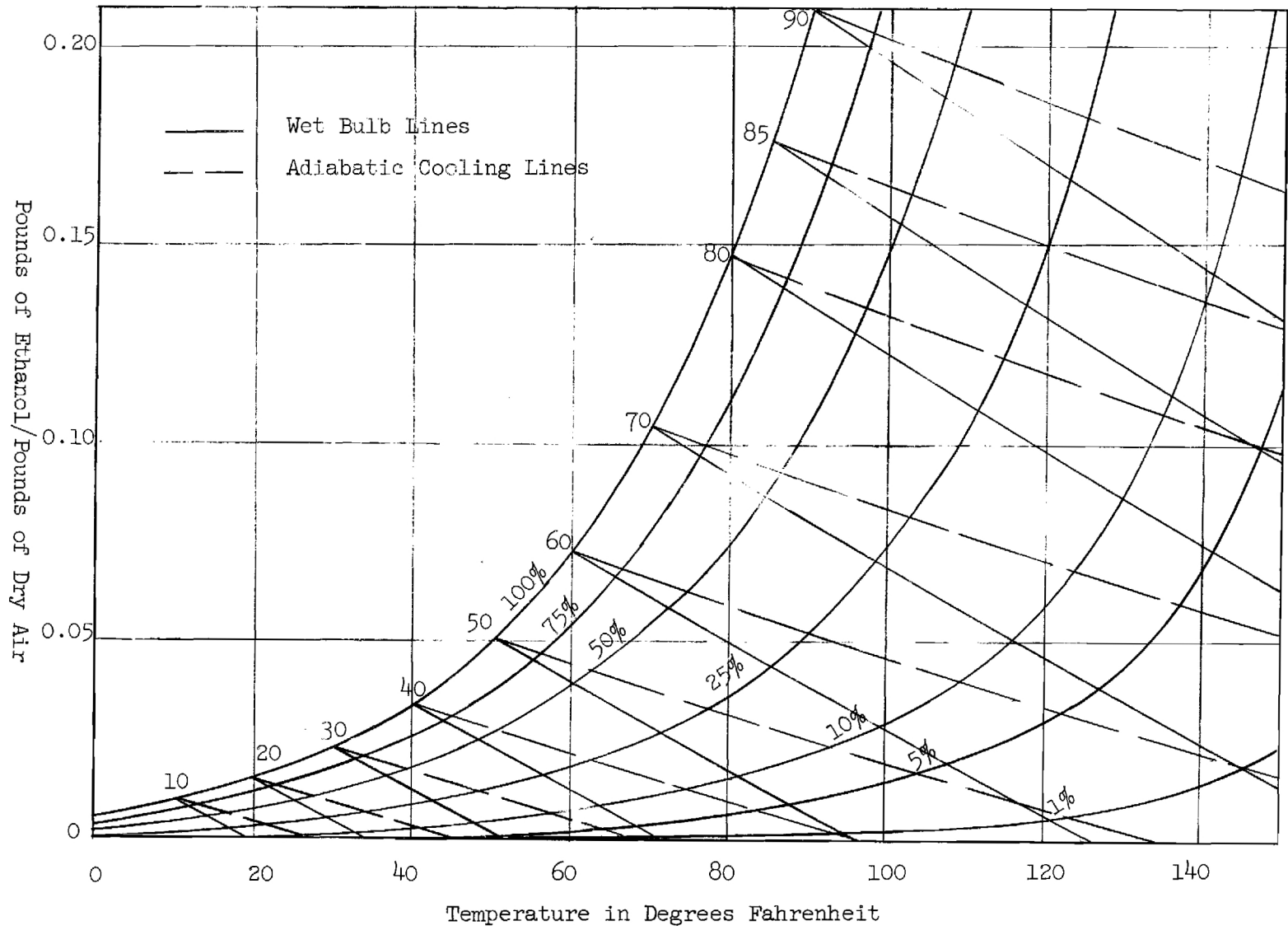
C. Tables of Data

X. APPENDIX

A. References

1. H. Köhler, "The Nucleus in and the Growth of Hygroscopic Droplets," Trans. Faraday Soc. 32, 1152-61 (1936).
2. C. Junge, "Das Grössenwachstum der Aitkenkerne," Ber. dent. Wetterdienstes, U. S.-Zone 38, 264-7 (1952).
3. V. K. LaMer and R. Gruen, "A Direct Test of Kelvin's Equation Connecting Vapor Pressure and Radius of Curvature," Trans Faraday Soc. 48, 410-15 (1952).
4. V. K. LaMer and S. Cotson, "The Growth and Shrinkage of Aerosols," Science 118, 516-7 (1953).
5. C. Orr, F. K. Hurd, W. P. Hendrix, and C. Junge, "The Behavior of Condensation Nuclei under Changing Humidities," J. Meteorology 15, 240-2 (1958).
6. C. Orr, F. K. Hurd, and W. J. Corbett, "Aerosol Size and Relative Humidity," J. Colloid Sci. 13, 472-82 (1958).
7. A. Goetz, "The Physics of Aerosols in the Submicron Range," Inhaled Particles and Vapours, p. 295-301, Pergamon Press, London, 1961.
8. C. Orr, F. K. Hurd, W. P. Hendrix, and W. J. Corbett, An Investigation into the Growth of Small Aerosol Particles with Humidity Change, Final Report, Project No. A-162, Georgia Tech Engineering Experiment Station, Atlanta, December 31, 1956.
9. E. A. Schuck and G. J. Doyle, Photo-oxidation of Hydrocarbons in Mixtures Containing Oxides of Nitrogen and Sulfur Dioxide, Report No. 29 Air Pollution Foundation, San Marino, California, October 1959.
10. F. K. Karioris and B. R. Fish, "An Exploding Wire Aerosol Generator," to be published in J. Colloid Sci.
11. R. Pearson and G. Langer, "Generation of Aerosols by Vapour-Phase Polymerization of Methyl Acrylate," Nature 187, 235 (July 16, 1960).
12. K. T. Whitby, A. R. McFarland, and D. A. Lundgren, Generator for Producing High Concentrations of Small Ions, Tech. Report No. 12, University of Minnesota, Minneapolis, July 1960.
13. C. N. Davies, "Definitive Equations for the Fluid Resistance of Spheres," Proc. Phys. Soc. 57, 259-70 (1945).
14. R. Tickner, unpublished report.

15. International Critical Tables 2, McGraw-Hill Book Co., Inc., New York, 1933, p. 149.
16. E. Guenther, The Essential Oils, Vol VI, D. Van Nostrand Co., Inc., New York, 1952.
17. Chemical Engineers Handbook (J.H. Perry, ed.) 3rd ed., McGraw-Hill Book Co., Inc., New York, 1950, p. 162.
18. A. Goetz, W. Stoeber, and T. Kallai, Synergistic Properties of Aerosols, Progress Report dated November 15, 1961, California Institute of Technology, Pasadena, California.



-85-

Figure 17. Psychrometric Chart for Ethanol in Air

TABLE XIII

CURRENT VERSUS VOLTAGE DATA OBTAINED FOR SYSTEMS OF STEARIC ACID AND ETHANOL

Volts	Current, x 10 ¹¹ Amperes, at Relative Humidities of Ethanol of									
	48%	57%	64%	69%	71%	75%	76%	77%	78%	79%
0	0	0	0	0	0	0	0	0	0	0
2	16.0	14.5	17.5	17.5	19.0	16.0	18.8	13.3	20.7	19.2
4	31.6	30.5	37.0	37.0	35.0	32.8	36.9	26.6	41.2	39.1
6	47.0	41.8	50.3	50.3	48.0	47.7	55.1	41.2	54.7	52.4
8	58.7	52.0	66.0	66.0	62.9	60.0	69.7	51.0	67.3	66.2
10	69.5	61.8	78.0	78.0	75.4	72.9	75.0	62.0	78.6	78.7
13	83.3	76.0	93.6	93.6	87.8	86.3	89.0	75.6	92.8	94.8
16	92.9	88.0	107.4	107.4	103.5	97.2	102.0	85.9	102.9	108.2
20	104.0	99.0	123.7	123.7	119.0	111.2	116.3	100.2	116.8	121.2
25	117.6	112.5	135.0	135.0	127.8	124.9	130.2	114.3	130.3	129.4
30	128.0	123.5	148.5	148.5	137.2	134.6	141.4	124.0	139.7	135.5
35	134.4	130.3	158.3	158.3	144.8	143.1	150.0	133.4	148.1	142.6
40	141.8	137.5	166.5	166.5	154.8	149.4	160.6	139.5	154.7	150.0
45	144.5	147.7	171.0	171.0	161.4	154.4	166.1	145.9	159.6	155.2
50	147.0	155.0	176.2	176.2	165.4	157.7	174.7	151.4	165.0	160.8
60	152.9	162.3	184.0	184.0	170.0	164.2	181.0	160.0	168.6	162.5
80	162.1	167.3	191.7	191.7	177.4	175.5	192.7	166.5	177.9	170.4
100	168.2	170.4	200.0	200.0	183.2	180.4	197.0	172.3	186.2	176.5
120	171.2	175.3	205.0	205.0	189.8	184.2	198.2	172.7	194.5	180.0
150	173.9	176.0	210.0	210.0	194.7	184.2	200.1	172.7	195.0	183.9
maximum	173.9	176.0	210.0	210.0	198.0	184.2	200.1	172.7	195.0	184.0

TABLE XIV

CURRENT VERSUS VOLTAGE DATA OBTAINED FOR SYSTEMS OF CAMPHOR AND ETHANOL

Volts	Current, x 10 ¹¹ Amperes, at Relative Humidities of Ethanol of								
	27%	35%	39%	54%	56%	68%	71%	91%	
0	0	0	0	0	0	0	0	0	
2	17	19	19	21	22	25	23	22	
5	43	40	45	43	50	48	48	41	
8	57	60	62	59	68	62	63	58	
10	64	68	72	67	76	67	70	64	
15	79	81	88	81	90	80	85	76	
20	89	92	99	--	97	89	--	--	
25	95	98	105	94	104	96	102	93	
35	102	106	114	102	113	101	110	101	
50	112	111	121	108	118	106	116	110	
75	115	114	124	113	123	110	121	116	
100	117	117	126	116	123	113	123	120	
120	117	--	127	--	124	114	123	--	
200	118	--	128	118	124	114	123	--	
maximum	118	120	128	118	124	114	123	124	

TABLE XV

CURRENT VERSUS VOLTAGE DATA OBTAINED FOR SYSTEMS
OF AMMONIUM IODIDE AND ETHANOL

Volts	Current, x 10 ¹¹ Amperes, at Relative Humidities of Ethanol of							
	23%	38%	41%	43%	53%	61%	67%	70%
0	0	0	0	0	0	0	0	0
2	13.4	12.9	13.0	11.9	12.1	8.1	8.5	5.9
4	28.0	24.7	26.0	25.1	24.4	17.3	14.1	8.9
6	40.3	37.0	38.0	35.7	36.2	27.8	19.8	14.0
8	50.5	47.8	48.0	47.2	46.8	36.8	25.8	22.0
10	61.3	56.9	58.0	59.0	57.5	44.2	32.4	20.4
13	75.2	71.7	70.0	72.2	71.0	55.6	41.3	27.6
16	86.9	83.9	79.5	83.6	83.6	65.7	51.0	35.9
20	99.8	95.2	90.0	95.1	97.6	76.3	61.2	45.9
25	115.3	108.6	101.5	109.6	112.9	88.3	72.9	53.8
30	125.8	120.7	111.0	121.7	126.0	101.3	86.6	63.2
35	134.7	130.7	119.0	130.8	135.5	111.0	95.9	--
40	143.3	138.5	124.5	140.4	145.5	121.2	105.8	70.2
45	149.8	144.1	129.5	146.0	154.0	130.2	113.1	--
50	155.8	151.1	134.0	152.7	159.9	138.8	122.1	94.6
55	159.8	--	137.2	--	164.0	146.2	130.2	--
60	162.7	156.8	140.1	160.0	168.2	151.0	134.2	108.1
70	166.7	162.9	145.0	167.0	173.9	154.1	144.3	120.1
80	169.6	167.6	148.2	169.0	179.5	161.2	151.3	129.1
100	174.1	169.6	152.0	176.1	185.1	169.7	165.4	140.2
120	179.5	174.9	154.5	178.1	190.2	177.0	169.0	147.5
150	179.8	176.9	156.0	182.4	196.1	182.8	178.8	162.8
maximum	179.8	176.9	158.0	182.4	199.0	185.0	184.0	168.9

TABLE XVI

CURRENT VERSUS VOLTAGE DATA OBTAINED FOR SYSTEMS OF STEARIC ACID AND TURPENTINE

Volts	Current, x 10 ¹¹ Amperes, at Weight Fractions of Turpentine of											
	0.0	0.285	0.381	0.368	0.437	0.481	0.521	0.555	0.561	0.580	0.581	0.600
0	0	0	0	0	0	0	0	0	0	0	0	0
5	18.6	18.5	21.0	18.5	19.8	22.2	17.7	22.2	18.0	17.8	14.3	18.5
10	29.1	37.9	44.8	36.8	40.9	48.0	34.3	45.3	35.8	36.8	28.6	37.9
15	55.2	55.9	64.9	56.9	60.0	66.9	49.9	64.1	51.7	54.1	39.9	55.9
20	67.9	70.3	87.1	71.0	75.2	85.0	63.4	78.9	65.0	65.9	48.5	70.3
25	78.5	82.8	96.4	85.3	90.3	99.8	75.1	89.9	76.1	77.0	58.0	82.8
30	86.9	92.2	109.1	97.0	101.6	113.1	83.7	100.0	85.0	86.2	65.2	92.2
35	94.3	101.6	121.4	107.6	111.9	123.1	91.5	108.1	91.8	93.8	73.9	101.6
40	101.0	109.7	130.1	118.4	123.0	133.1	98.8	115.2	98.6	99.4	79.6	109.7
45	106.5	116.3	138.4	125.5	129.6	140.4	105.0	118.9	104.0	105.6	86.0	116.3
50	111.0	122.3	145.9	133.0	138.6	147.9	111.1	123.1	108.9	110.0	91.6	122.3
60	117.9	130.4	155.9	143.3	147.2	159.3	121.0	128.7	116.9	117.6	99.5	130.4
70	123.5	137.5	164.5	152.8	156.8	165.9	127.8	132.0	122.9	124.9	105.6	137.5
80	126.1	143.2	168.5	158.5	163.0	171.0	133.2	134.8	126.1	129.2	110.0	143.2
90	--	--	172.5	164.7	166.0	174.1	137.3	--	--	132.8	--	--
100	133.2	148.0	175.0	168.7	170.1	179.8	141.3	137.0	133.0	133.1	116.7	148.0
120	138.7	154.5	177.8	172.2	174.9	184.7	146.2	138.9	134.7	134.0	123.2	154.5
150	139.8	156.2	186.9	175.4	180.1	189.8	150.7	140.7	137.9	135.3	127.7	146.2
200	141.3	156.7	188.7	182.9	182.8	196.9	156.0	141.6	139.3	136.2	127.7	156.7
maximum	141.3	156.7	188.7	183.0	182.8	196.9	157.1	141.6	139.3	136.2	127.7	156.7

TABLE XVII

CURRENT VERSUS VOLTAGE READINGS OBTAINED FOR SYSTEMS
OF AMMONIUM IODIDE AND DIOCTYLPHthalate

Volts	Current, x 10 ¹¹ Amperes, at Vapor Concentrations Obtained from Bath Temperatures of				
	No Dioctylphthalate	28.8°C	35.0°C	48.1°C	73.2°C
0	0	0	0	0	0
5	14.1	15.3	17.7	15.7	16.8
10	28.1	31.1	29.8	30.0	31.1
15	42.0	44.8	45.0	43.6	44.0
20	54.3	57.0	55.0	56.0	56.0
25	63.1	69.3	65.3	67.0	67.2
30	73.0	79.3	74.7	76.7	76.2
35	80.8	88.8	81.6	85.6	85.8
40	86.3	97.2	87.0	94.0	92.9
50	97.0	109.0	100.0	104.6	105.8
60	105.6	122.1	107.0	115.0	114.7
70	111.6	128.0	112.7	119.8	123.3
80	118.4	133.2	119.0	123.6	133.3
100	123.5	138.1	123.7	132.0	139.0
120	129.1	143.0	127.0	136.0	143.0
150	132.1	143.7	130.0	140.0	149.0
200	132.1	145.0	134.0	141.8	152.2
maximum	132.1	145.0	134.0	141.8	152.2

TABLE XVIII
CURRENT VERSUS VOLTAGE DATA FOR SYSTEMS
OF PARAFFIN AND HEXANE

Volts	Current, $\times 10^{11}$ Amperes, at Hexane Bath Temperatures of		
	24.6°C	47.8°C	76.3°C
0	0	0	0
2	10.7	12.8	19.2
4	15.6	17.2	26.4
6	20.0	22.2	34.3
8	25.3	27.8	44.1
10	30.5	33.5	51.1
13	38.8	42.1	--
16	45.8	49.0	70.6
20	54.9	57.4	80.7
25	64.0	65.9	89.0
30	71.1	72.9	96.2
35	76.0	78.5	102.5
40	80.4	83.1	107.3
45	84.7	--	--
50	86.0	88.9	114.1
60	88.8	92.1	119.8
70	91.0	93.9	--
80	92.0	95.0	123.0
100	93.0	96.0	123.7
maximum	93.0	96.0	123.7

TABLE XIX

CURRENT VERSUS VOLTAGE DATA OBTAINED FOR SYSTEMS
OF NAPHTHALENE AND GASOLINE

Volts	Current, x 10 ¹¹ Amperes, at Gasoline Temperatures of					
	24.0°C	25.1°C	31.5°C	37.2°C	54.6°C	60.0°C
0	0	0	0	0	0	0
2	25.0	22.0	23.0	30.0	25.0	16.1
4	45.9	33.5	43.5	52.0	46.5	30.5
6	60.8	46.0	62.0	70.0	65.0	44.5
8	74.0	58.3	76.5	84.0	80.9	57.2
10	83.9	63.9	87.8	94.9	100.5	69.3
13	95.5	75.1	102.0	107.8	113.3	86.0
16	105.0	84.2	112.0	117.2	128.0	100.0
20	113.9	95.2	122.1	126.1	140.9	122.8
25	120.3	103.4	128.8	134.3	156.5	130.9
30	124.9	109.0	134.4	136.1	168.9	137.0
35	127.0	110.8	139.8	141.1	170.7	--
40	128.3	113.5	141.2	142.7	173.2	152.3
50	130.2	114.8	142.8	144.0	175.6	158.1
60	131.6	115.5	145.7	145.4	175.7	160.9
80	131.6	115.5	148.8	145.8	175.7	162.6
maximum	131.6	115.5	148.8	145.8	175.7	162.6

TABLE XX

CURRENT VERSUS VOLTAGE DATA OBTAINED FOR SYSTEMS OF POLY(METHYL METHACRYLATE)
AND METHYL ETHYL KETONE

Volts	Current, $\times 10^{11}$ Amperes, at Relative Humidities of Ketone of									
	Test 1		Test 2		Test 3		Test 4		Test 5	
	0%	33%	0%	34%	0%	48%	0%	55%	0%	75%
0	0	0	0	0	0	0	0	0	0	0
2	18.0	16.0	12.2	7.0	19.0	12.7	10.0	3.6	19.2	19.0
4	25.5	25.0	20.0	15.5	23.3	22.0	19.0	8.2	30.0	24.0
6	30.8	33.3	26.6	21.8	30.2	30.0	25.8	11.0	35.2	27.0
8	33.2	37.6	27.5	26.2	32.5	33.5	30.7	14.0	38.0	35.0
10	34.6	42.1	29.3	28.7	34.2	38.8	33.8	18.7	41.0	40.0
13	37.8	45.8	33.3	32.0	36.3	41.7	37.8	21.2	42.0	50.0
16	40.2	48.7	39.3	37.0	36.3	44.1	39.0	28.0	45.0	57.2
20	41.5	49.0	43.2	40.8	38.7	49.9	40.3	29.5	47.3	60.0
25	44.5	--	50.0	44.0	--	55.8	43.7	33.0	--	61.4
30	44.7	54.4	53.0	48.8	41.0	60.0	44.8	34.7	50.0	64.2
40	45.0	48.0	55.0	53.1	--	61.0	45.0	36.0	--	70.2
50	--	48.7	55.2	--	42.1	--	45.0	39.0	50.6	72.8
60	45.0	48.8	--	58.2	--	66.8	45.0	40.5	--	73.8
80	--	--	--	60.0	--	70.0	--	--	--	75.8
100	--	--	--	60.0	--	70.0	--	42.0	--	--
maximum	45.0	58.8	55.2	60.0	--	70.0	45.0	42.0	50.6	78.0

(Continued)

TABLE XX (Concluded)

CURRENT VERSUS VOLTAGE DATA OBTAINED FOR SYSTEMS OF POLY(METHYL METHACRYLATE)
AND METHYL ETHYL KETONE

Volts	Current, x 10 ¹¹ Amperes, at Relative Humidities of Ketone of									
	Test 6		Test 7		Test 8		Test 9		Test 10	
	0%	43%	0%	47%	0%	54%	0%	60%	0%	67%
0	0	0	0	0	0	0	0	0	0	0
2	10.0	6.5	20.2	7.0	10.5	2.8	42.2	14.8	31.0	12.1
4	15.5	11.0	33.2	12.0	20.8	5.2	61.3	27.5	46.5	18.0
6	20.6	18.7	46.0	18.7	29.0	8.0	74.7	38.5	52.8	21.8
8	23.7	24.7	59.8	19.7	36.0	9.7	85.3	47.5	60.0	27.7
10	26.0	27.8	69.3	21.0	36.5	11.0	89.4	55.0	62.2	30.3
13	29.7	31.0	77.8	22.9	45.0	14.0	97.0	64.4	64.0	39.5
16	32.8	35.6	85.5	27.0	47.0	15.7	102.6	71.8	71.1	44.3
20	36.2	39.8	94.0	31.0	48.8	17.8	105.5	80.0	74.5	47.5
25	40.5	42.0	101.6	33.2	50.5	20.0	107.5	88.0	75.5	51.3
30	43.5	43.3	109.0	36.2	51.8	22.0	110.9	92.8	--	54.7
40	43.5	47.5	109.3	40.0	53.2	25.3	113.0	99.4	--	57.0
50	--	50.0	109.3	41.9	54.0	28.3	113.0	103.0	75.5	--
60	43.5	51.4	109.3	48.7	54.5	30.7	--	106.5	--	59.0
80	--	53.4	--	54.2	54.5	33.5	--	109.5	--	60.0
100	--	54.0	--	54.2	--	--	--	110.0	--	62.0
maximum	43.5	54.0	109.3	54.2	54.5	35.0	113.0	110.0	75.5	62.0